Non-perturbative QCD aspects of elastic hadronic scatterings*

Mateus Broilo da Rocha

Federal University of Rio Grande do Sul

Doctor qualifying exam

Supervisor: Prof. Dr. Emerson Gustavo de Souza Luna

*This research was supported by CNPq grant 141496/2015-0.

Outline

- Mini-introduction
  - Experimental data
  - Quick inspection on kinematics
  - Eikonal formalism
- Regge-Gribov based model
  - Regge theory
  - Phenomenology
  - Results so far
- QCD-inspired model
  - Quantum Chromodynamics
  - QIM formalism
  - Results so far
- Perspectives

Introduction

- The study of hadron-hadron total cross-sections has been a subject of intense theoretical and experimental interest

- The recent measurements of pp elastic, inelastic and total cross-sections at the LHC by the TOTEM Collaboration

$\Rightarrow$ have enhanced the interest in the subject

$\Rightarrow$ have become a pivotal source of information for selecting models and theoretical methods

- At present QCD-inspired formalism is one of the main theoretical approaches used to describe the observed increase of σ_{tot}^{hh}

- However, the recent LHC data provides a unique constraint on the soft Pomeron parameters

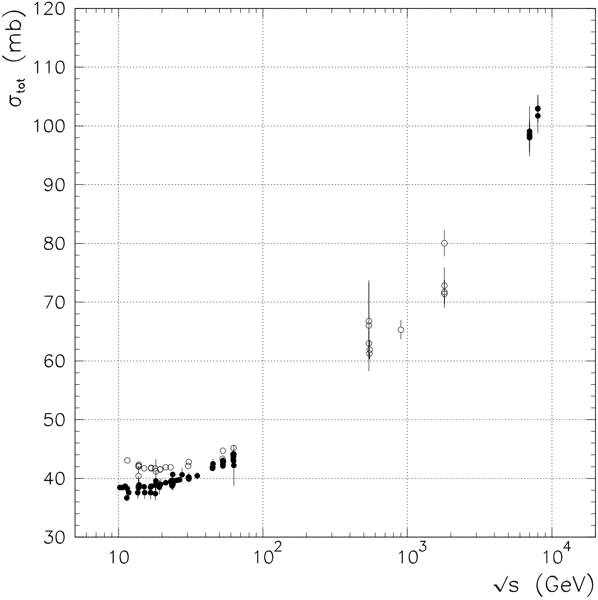

Total cross-section data for pp (•) and $\bar{p}$p (○) scattering.

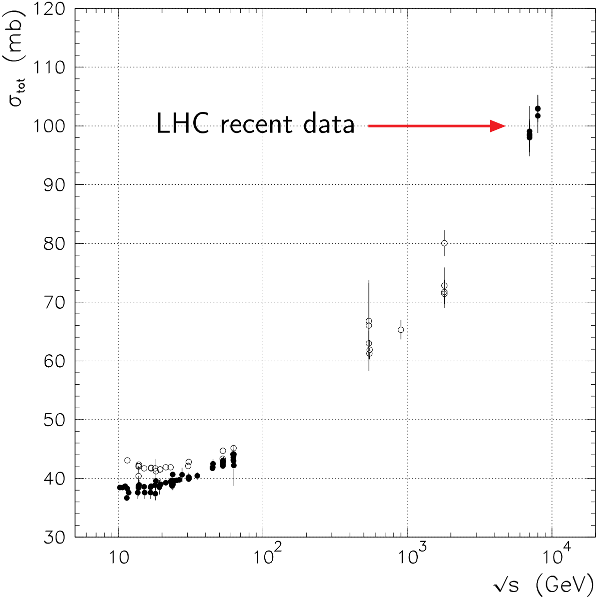

Total cross-section data for pp (●) and $\bar{p}p$ (○) scattering.

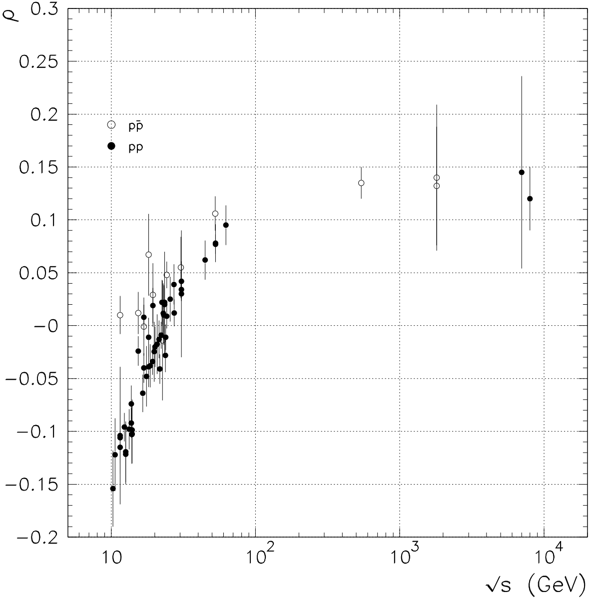

Ratio of the real to imaginary part of the forward scattering amplitude.

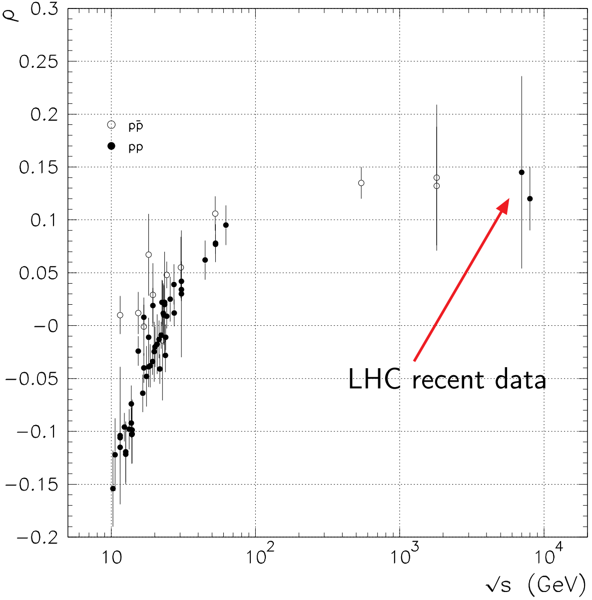

Ratio of the real to imaginary part of the forward scattering amplitude.

Experimental data

Collaboration	Reference	$\sqrt{s}$ (TeV)	σ_{tot} (mb)
TOTEM	EPL96 (2011) 21002	7	98.30 ± 2.80
	EPL101 (2013) 21002	7	98.58 ± 2.23
	EPL101 (2013) 21004	7	99.10 ± 4.30
	EPL101 (2013) 21004	7	98.00 ± 2.50
	PRL111 (2013) 012001	8	101.70 ± 2.90
	EPJ C76 (2016) 661	8	102.90 ± 2.30
	EPJ C76 (2016) 661	8	103.00 ± 2.30

Collaboration	Reference	$\sqrt{s}$ (TeV)	ρ
TOTEM	EPL101 (2013) 21002	7	0.145 ± 0.091
TOTEM	EPJ C76 (2016) 661	8	0.120 ± 0.030

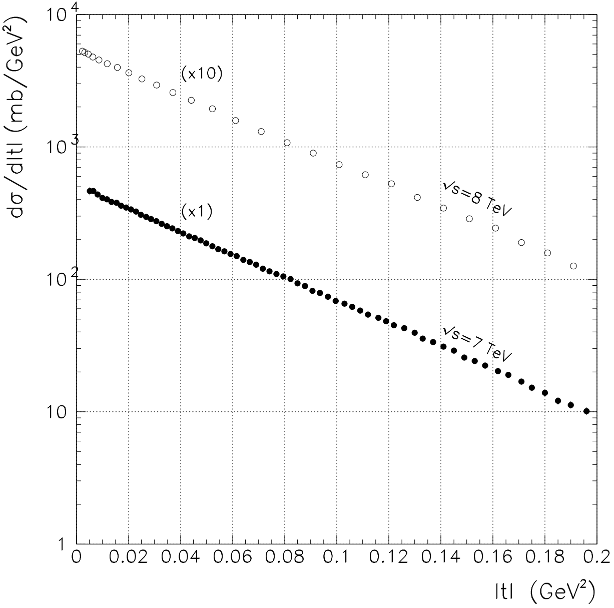

Elastic pp differential cross-section.

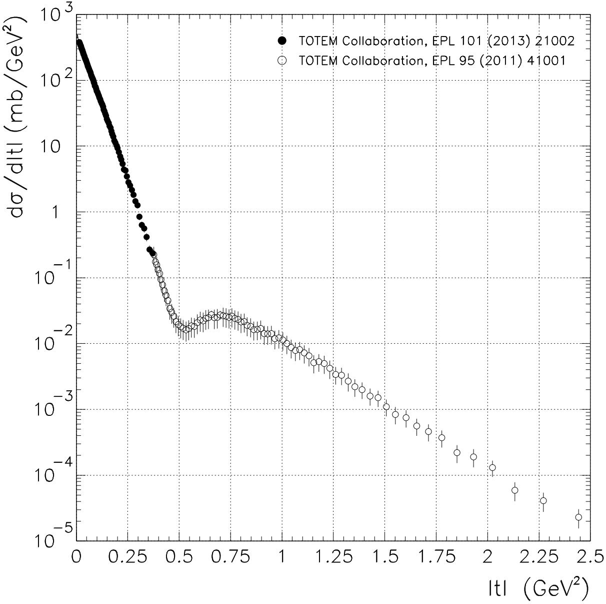

Elastic pp differential cross-section at $\sqrt{s} = 7$ TeV.

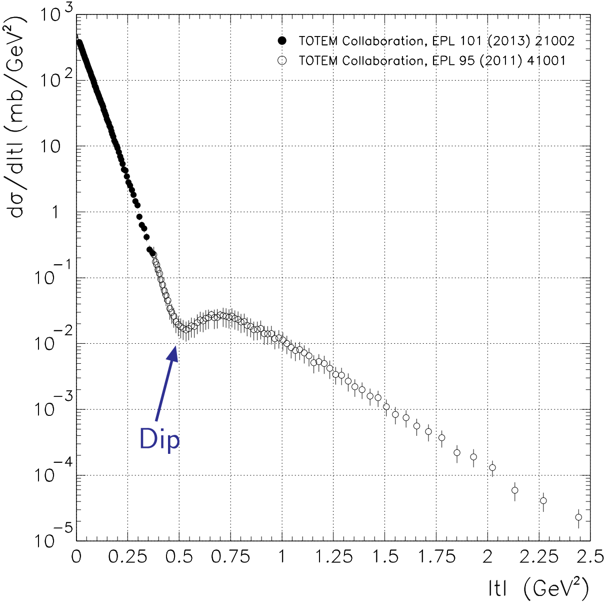

Elastic pp differential cross-section at $\sqrt{s} = 7$ *TeV.*

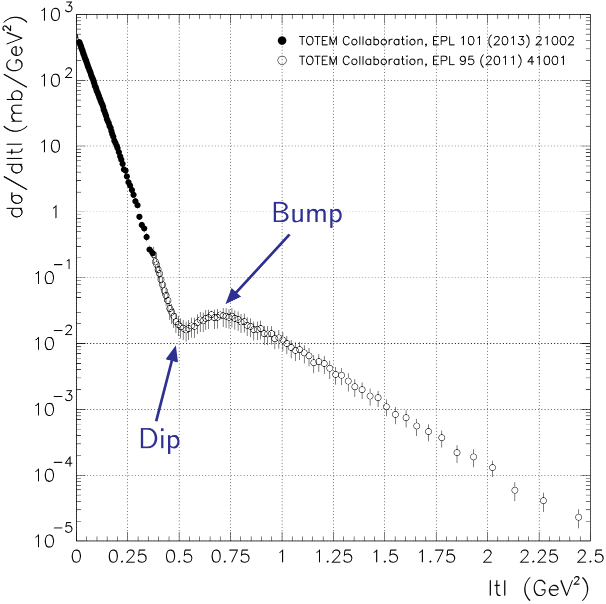

Elastic pp differential cross-section at $\sqrt{s} = 7$ *TeV.*

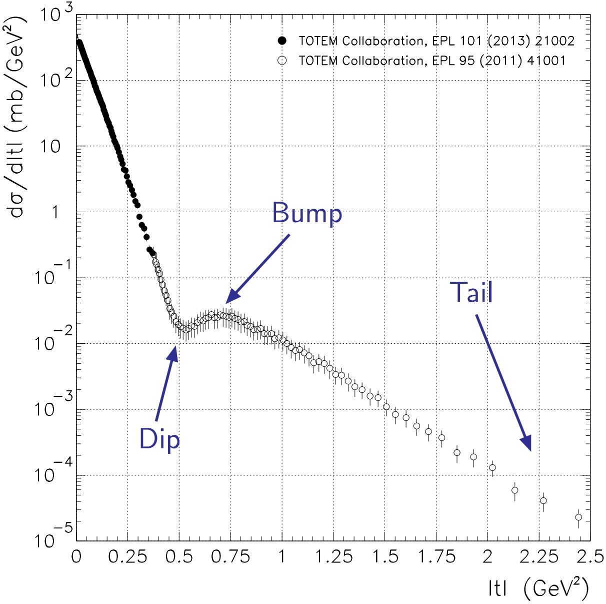

Elastic pp differential cross-section at $\sqrt{s} = 7$ *TeV.*

Quick inspection on kinematics

- Collisions lead to scatterings

$$1 + 2 \to 3 + 4 + 5 + \ldots$$

- Two-body exclusive process

$$1 + 2 \to 3 + 4 \quad (s\text{-channel})$$

- Mandelstam invariants

$$s = (P_1 + P_2)^2 = (P_3 + P_4)^2$$
$$t = (P_1 - P_3)^2 = (P_2 - P_4)^2$$
$$u = (P_1 - P_4)^2 = (P_2 - P_3)^2$$

constrained to

$$s + t + u = \sum_{i=1}^{4} m_i^2$$

Quick inspection on kinematics

- In the crossed channel (time-reversed)

$$1 + \bar{3} \to \bar{2} + 4 \;\; (t\text{-channel})$$

- By crossing-symmetry

$$F_{1+2\to3+4}(s,t,u) = F_{1+\bar{3}\to\bar{2}+4}(t,s,u)$$

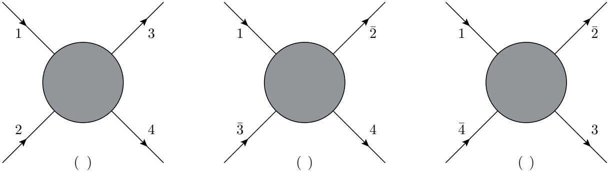

Quick inspection on kinematics

- Elastic scattering: the incident particles corresponds exactly to those ones in the final state.

$$1 + 2 \rightarrow 1' + 2'$$

- Simplest kinematic processes $\rightarrow$ theoretical description is extremely difficult.

- Elastic pp and $\bar{p}p$ scattering

$$s-\text{channel}: \quad p + p \rightarrow p + p$$

$$t-\text{channel}: \quad \bar{p} + p \rightarrow \bar{p} + p$$

Eikonal formalism

- Partial-wave approximation

$$f(\mathbf{k},\mathbf{k}') = f(k,\theta) = \sum_{\ell=0}^{\infty}(2\ell+1)\, a_\ell(k) P_\ell(\cos\theta)$$

- By taking the high-energy limit

$$f(s,t) = ik \int_0^\infty db\, b\, J_0(b\sqrt{-t}) \underbrace{\left[1 - e^{i\chi(s,b)}\right]}_{\equiv \Gamma(s,b)}$$

- Unitarity condition

$$\Gamma(s,b) = \mathrm{Re}\,\Gamma(s,b) + i\mathrm{Im}\,\Gamma(s,b)$$

$$2\mathrm{Re}\,\Gamma(s,b) = |\Gamma(s,b)|^2 + (1 - e^{-2\chi_I})$$

Eikonal formalism

- Total cross-section

$$\sigma_{tot}(s) = 2\pi \int_0^\infty db\, b\, 2\, \mathrm{Re}\Gamma(s,b)$$
$$= 4\pi \int_0^\infty db\, b\, [1 - e^{-\chi_I} \cos\chi_R] = \sigma_{el} + \sigma_{in}$$

- Elastic differential cross-section

$$\frac{d\sigma}{dt}(s,t) = \pi \left| i \int_0^\infty db\, b\, J_0(b\sqrt{-t}) \left[1 - e^{i\chi(s,b)}\right] \right|^2$$

- ρ-parameter

$$\rho(s) = \frac{\mathrm{Re}\left\{ i \int_0^\infty db\, b\, [1 - e^{i\chi(s,b)}] \right\}}{\mathrm{Im}\left\{ i \int_0^\infty db\, b\, [1 - e^{i\chi(s,b)}] \right\}} = \frac{\int_0^\infty db\, b\, e^{-\chi_I} \sin\chi_R}{\int_0^\infty db\, b\, \left(1 - e^{-\chi_I} \cos\chi_R\right)}$$

Regge theory

Regge theory: Basics

- The Regge pole idea $\rightarrow$ strong interaction is described by the exchange of Regge trajectories

- Each pole corresponds to singularities in the partial-wave amplitude

$$\ell = \alpha(t)$$

– $\alpha(t)$ stands for the Regge trajectory

- At high-energy

$$A(s,t) \underset{s\to\infty}{\sim} s^{\alpha(t)}$$

- Asymptotically the Pomeron dominates at high energies, whereas the secondary Reggeons are responsible for the low-energy region

- **Fundamental result:**

Regge theory: Basics

- The Regge pole idea $\rightarrow$ strong interaction is described by the exchange of Regge trajectories

- Each pole corresponds to singularities in the partial-wave amplitude

$$\ell = \alpha(t)$$

– $\alpha(t)$ stands for the Regge trajectory

- At high-energy

$$A(s,t) \underset{s\rightarrow\infty}{\sim} s^{\alpha(t)}$$

- Asymptotically the Pomeron dominates at high energies, whereas the secondary Reggeons are responsible for the low-energy region

- **Fundamental result:** the leading complex angular momentum singularity of the partial-wave amplitude in a given channel, determines the asymptotic behaviour of the scattering amplitude in the crossed channels

Regge theory: Basics

- The Regge pole idea $\rightarrow$ strong interaction is described by the exchange of Regge trajectories
- Each pole corresponds to singularities in the partial-wave amplitude

$$\ell = \alpha(t)$$

– $\alpha(t)$ stands for the Regge trajectory

- At high-energy

$$A(s,t) \underset{s\rightarrow\infty}{\sim} s^{\alpha(t)}$$

- Asymptotically the Pomeron dominates at high energies, whereas the secondary Reggeons are responsible for the low-energy region
- **Fundamental result:** the ~~leading complex angular momentum singularity~~ **Regge pole** of the partial-wave amplitude in a given channel, determines the asymptotic behaviour of the scattering amplitude in the crossed channels

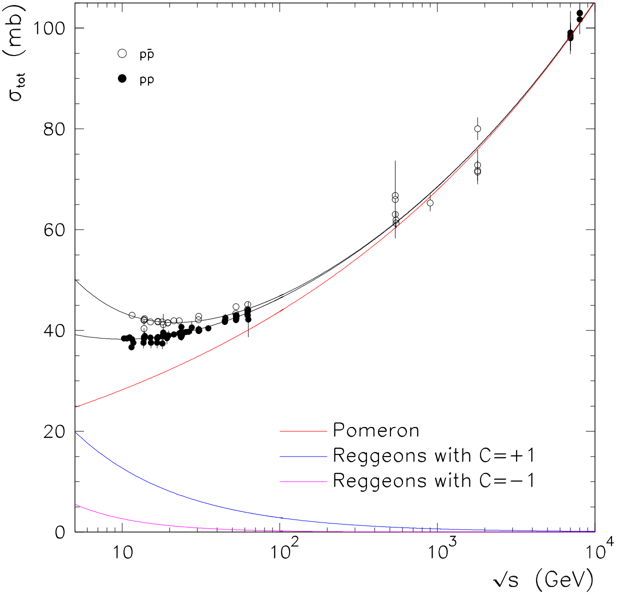

Simple Regge-Gribov based model. Contribution from each Reggeon amplitude at the Born-level, respectively.

Regge theory: Regge poles → Long story short

- The scattering amplitude is written as the **Watson-Sommerfeld** transform of the partial-wave series
  – The dominant contribution in the case of t-channel exchange

$$A(s,t) \underset{s\to\infty}{\simeq} \sum_{\xi=\pm 1} \sum_{i_\xi} -\gamma_{i_\xi}(t) \frac{1+\xi e^{-i\pi\alpha_{i_\xi}(t)}}{\sin \pi\alpha_{i_\xi}(t)} s^{\alpha_{i_\xi}(t)}$$

  – α_{i_ξ} defines the location of the i-th pole → each Reggeon contribution
  – $\gamma_{i_\xi}(t)$ stands for the residue function and *phenomenologically* is related to the vertex coupling hadron-Reggeon
- Leading pole → **Pomeron** $\xi = +1$

$$A(s,t) \underset{s\to\infty}{\sim} -\gamma_i(t) \frac{1+\xi e^{-i\pi\alpha(t)}}{\sin \pi\alpha(t)} s^{\alpha(t)}$$

- New quantum number, the signature $\xi = \pm 1$
  – Then $A_\ell(t)$ can be analytically continued to complex ℓ-values by means of the **Watson-Sommerfeld transform**

Phenomenology

- Returning to the task in hand (**description of pp and $\bar{p}p$ scatterings**)...
  But beforehand:
  - diffractive processes are described by Regge theory
  - high-energy behaviour of the scattering amplitude $\rightarrow$ described by singularities of the amplitude in the **complex angular momentum plane**
- As it was previously mentioned

$$A(s,t) \propto s^{\alpha(t)}$$

- If more than one pole contributes

$$A(s,t) = \sum_i \gamma_i(t)\eta_i(t)s^{\alpha_i(t)}$$

  - where $\eta_i(t) = -\frac{1+\xi e^{-i\pi\alpha_i(t)}}{\sin(\pi\alpha_i(t))}$ is the signature factor
- Straightforward

Phenomenology

- Returning to the task in hand (**description of pp and $\bar{p}p$ scatterings**)... But beforehand:
  - diffractive processes are described by Regge theory
  - high-energy behaviour of the scattering amplitude $\rightarrow$ described by singularities of the amplitude in the **complex angular momentum plane**
- As it was previously mentioned

$$A(s,t) \propto s^{\alpha(t)}$$

- If more than one pole contributes

$$A(s,t) = \sum_i \gamma_i(t)\eta_i(t)s^{\alpha_i(t)} \text{ (as it was also mentioned)}$$

  - where $\eta_i(t) = -\frac{1+\xi e^{-i\pi\alpha_i(t)}}{\sin(\pi\alpha_i(t))}$ is the signature factor
- Straightforward

Phenomenology

- Returning to the task in hand (**description of pp and $\bar{p}p$ scatterings**)... But beforehand:
  – diffractive processes are described by Regge theory
  – high-energy behaviour of the scattering amplitude $\rightarrow$ described by singularities of the amplitude in the **complex angular momentum plane**
- As it was previously mentioned

$$A(s,t) \propto s^{\alpha(t)}$$

- If more than one pole contributes

$$A(s,t) = \sum_i \gamma_i(t)\eta_i(t)s^{\alpha_i(t)} \quad \text{(as it was also mentioned)}$$

– where $\eta_i(t) = -\frac{1+\xi e^{-i\pi\alpha_i(t)}}{\sin(\pi\alpha_i(t))}$ is the signature factor

- Straightforward

$$\eta(t) = \underbrace{-\frac{e^{-i\pi\alpha_i(t)/2}}{\sin\left(\frac{\pi}{2}\,\alpha_i(t)\right)}}_{\xi=+1}$$

Phenomenology

- Returning to the task in hand (**description of pp and $\bar{p}p$ scatterings**)...
  But beforehand:
  – diffractive processes are described by Regge theory
  – high-energy behaviour of the scattering amplitude $\rightarrow$ described by singularities of the amplitude in the **complex angular momentum plane**
- As it was previously mentioned

$$A(s,t) \propto s^{\alpha(t)}$$

- If more than one pole contributes

$$A(s,t) = \sum_i \gamma_i(t)\eta_i(t)s^{\alpha_i(t)} \quad \text{(as it was also mentioned)}$$

– where $\eta_i(t) = -\frac{1+\xi e^{-i\pi\alpha_i(t)}}{\sin(\pi\alpha_i(t))}$ is the signature factor

- Straightforward

$$\eta(t) = \underbrace{-\frac{e^{-i\pi\alpha_i(t)/2}}{\sin\left(\frac{\pi}{2}\,\alpha_i(t)\right)}}_{\xi=+1} \quad \text{and} \quad \eta(t) = \underbrace{-i\,\frac{e^{-i\pi\alpha_i(t)/2}}{\cos\left(\frac{\pi}{2}\,\alpha_i(t)\right)}}_{\xi=-1}$$

Phenomenology: Born-level analysis

- The scattering amplitude is decomposed into three terms

$$A_B(s,t) = A_{\mathbb{P}}(s,t) + A_+(s,t) + \tau\, A_-(s,t)$$

where τ flips sign when going from $\underline{pp\,(\tau=-1)}$ to $\underline{\bar{p}p\,(\tau=+1)}$

- leading singularity:

– $A_{\mathbb{P}}(s,t) \rightarrow$ single **Pomeron** exchange, $\xi = +1$

- secondary Reggeons:

– $A_{+(-)}(s,t) \rightarrow$ exchange of the Reggeons with $\xi = +1(-1)$, namely a_2 and f_2 (ω and ρ)

- For single Regge exchange

$$A_i(s,t) = \beta_i^2(t)\eta_i(t)\left(\frac{s}{s_0}\right)^{\alpha_i(t)}$$

– where $\gamma_i(t) = \beta_i^2(t)$ is the elastic proton-Reggeon vertex, $\alpha_i(t)$ is the Regge pole trajectory, with $i = \mathbb{P}, +, -$

Phenomenology: Born-level analysis

- Asymptotic form of the signatures at the very **low-t region**

Phenomenology: Born-level analysis

- Asymptotic form of the signatures at the very **low-t region**

$$\eta_i(t) = \underbrace{-e^{-i\pi\alpha_i(t)/2}}_{\xi=+1}$$

Phenomenology: Born-level analysis

- Asymptotic form of the signatures at the very **low-t region**

$$\eta_i(t) = \underbrace{-e^{-i\pi\alpha_i(t)/2}}_{\xi=+1} \quad \text{and} \quad \eta_i(t) = \underbrace{ie^{-i\pi\alpha_i(t)/2}}_{\xi=-1}$$

Phenomenology: Born-level analysis

- Asymptotic form of the signatures at the very **low-t region**

$$\eta_i(t) = \underbrace{-e^{-i\pi\alpha_i(t)/2}}_{\xi=+1} \quad \text{and} \quad \eta_i(t) = \underbrace{ie^{-i\pi\alpha_i(t)/2}}_{\xi=-1}$$

- do not affect the Pomeron parameters ϵ and $\alpha'_{\mathbb{P}}$, but simply introduces the vertex transformations

$$\beta^2_{\mathbb{P}}(t) \to \sin\left(\frac{\pi}{2}\alpha_{\mathbb{P}}(t)\right)\beta^2_{\mathbb{P}}(t),$$
$$\beta^2_{+}(t) \to \sin\left(\frac{\pi}{2}\alpha_{+}(t)\right)\beta^2_{+}(t),$$
$$\beta^2_{-}(t) \to -\cos\left(\frac{\pi}{2}\alpha_{-}(t)\right)\beta^2_{-}(t).$$

Phenomenology: Born-level analysis

By means of these simplified form of the Regge signatures:

- **Pomeron contribution, $\xi = +1$**

$$A_{\mathbb{P}}(s,t) = -\beta_{\mathbb{P}}^2(t)\cos\left(\frac{\pi}{2}\alpha_{\mathbb{P}}(t)\right)\left(\frac{s}{s_0}\right)^{\alpha_{\mathbb{P}}(t)} + i\beta_{\mathbb{P}}^2(t)\sin\left(\frac{\pi}{2}\alpha_{\mathbb{P}}(t)\right)\left(\frac{s}{s_0}\right)^{\alpha_{\mathbb{P}}(t)}$$

- **Reggeons with $\xi = +1$**

$$A_{+}(s,t) = -\beta_{+}^2(t)\cos\left(\frac{\pi}{2}\alpha_{+}(t)\right)\left(\frac{s}{s_0}\right)^{\alpha_{+}(t)} + i\beta_{+}^2(t)\sin\left(\frac{\pi}{2}\alpha_{+}(t)\right)\left(\frac{s}{s_0}\right)^{\alpha_{+}(t)}$$

- **Reggeons with $\xi = -1$**

$$A_{-}(s,t) = \beta_{-}^2(t)\sin\left(\frac{\pi}{2}\alpha_{-}(t)\right)\left(\frac{s}{s_0}\right)^{\alpha_{-}(t)} + i\beta_{-}^2(t)\cos\left(\frac{\pi}{2}\alpha_{-}(t)\right)\left(\frac{s}{s_0}\right)^{\alpha_{-}(t)}$$

Phenomenology: Born-level analysis

Secondary Reggeons exchange

- Positive-signature are taken to have an exponential form for the proton-Reggeon vertex

$$\beta_+(t) = \beta_+(0)\exp(r_+ t/2)$$

– lie on an exchange-degenerate linear trajectory

$$\alpha_+(t) = 1 - \eta_+ + \alpha'_+ t$$

- Similarly, for the case of the exchange-degenerate negative-signature

$$\beta_-(t) = \beta_-(0)\exp(r_- t/2)$$

$$\alpha_-(t) = 1 - \eta_- + \alpha'_- t$$

Phenomenology: Born-level analysis

Pomeron exchange

it will be investigated two different types of:

- **proton-Pomeron vertex**, (one of which being a power-like form):

$$\beta_{\mathbb{P}}(t) = \beta_{\mathbb{P}}(0)\exp(r_{\mathbb{P}}t/2) \quad \text{and} \quad \beta_{\mathbb{P}}(t) = \frac{\beta_{\mathbb{P}}(0)}{(1-t/a_1)(1-t/a_2)}$$

- **trajectories**, (one of which being non-linear):

$$\alpha_{\mathbb{P}}(t) = \alpha_{\mathbb{P}}(0) + \alpha'_{+}t \quad \text{and} \quad \alpha_{\mathbb{P}}(t) = \alpha_{\mathbb{P}}(0) + \alpha'_{\mathbb{P}}t - \frac{\beta_{\pi}^2 m_{\pi}^2}{32\pi^3}\, h\left(\frac{4m_{\pi}^2}{|t|}\right)$$

$$h(x) = \frac{4}{x}F_{\pi}^2(t)\left[2x - (1+x)^{3/2}\ln\left(\frac{\sqrt{1+x}+1}{\sqrt{1+x}-1}\right) + \ln\left(\frac{m^2}{m_{\pi}^2}\right)\right]$$

– non-linear term $\rightarrow$ nearest t-channel singularity (two-pion loop)

– $m_{\pi} = 139.6$ MeV and $F_{\pi}(t) = \beta_{\pi}/(1-t/a_1)$ stands for the pion-Pomeron vertex

– $\beta_{\pi}/\beta_{\mathbb{P}} = 2/3$

Phenomenology: Born-level analysis

- **BI model**:

  – it was adopted an exponential form for the proton-Pomeron vertex and for the secondary Reggeons

  – it was used a ***linear trajectory*** for the Pomeron

- **BII model**:

  – exponential form for the proton-Pomeron vertex and for the secondary Reggeons

  – ***non-linear trajectory*** for the Pomeron

- **BIII model**:

  – power-like form for the proton-Pomeron vertex and exponential form for the secondary Reggeons

  – ***non-linear trajectory*** for the Pomeron

- **BIV(=BI+$\mathbb{PP}$) model** (double-Pomeron exchange):

  – power-like form for the proton-Pomeron vertex and for the secondary Reggeons

  – ***non-linear trajectory*** for the Pomeron

Phenomenology: Born-level analysis

Double-Pomeron exchange

– **multi-Pomeron exchanges** tame the asymptotic rise of cross-section $\rightarrow$ enters, phenomenologically, to ensure unitarity

- $\mathbb{P}\mathbb{P}$ contribution is negative, at $s \rightarrow \infty$ as $A_{\mathbb{P}\mathbb{P}}(s,t) \sim -s^{\alpha_{\mathbb{P}\mathbb{P}}(t)} / \ln s$
- is flatter in t than the single-Pomeron exchange

$$\alpha_{\mathbb{P}\mathbb{P}}(t) = 1 + 2\epsilon + \frac{1}{2}\,\alpha'_{\mathbb{P}}\,t$$

- it was added the phenomenological term to the amplitude

$$A_{\mathbb{P}\mathbb{P}}(s,t) = -\beta^2_{\mathbb{P}\mathbb{P}}(t)\,\eta_{\mathbb{P}\mathbb{P}}(t)\,\frac{s}{s_0}^{\alpha_{\mathbb{P}\mathbb{P}}(t)}\left[\ln\left(-i\,\frac{s}{s_0}\right)\right]^{-1}$$

– where $\eta_{\mathbb{P}\mathbb{P}}(t) = -e^{-i\pi\alpha_{\mathbb{P}\mathbb{P}}(t)/2}$, $\beta_{\mathbb{P}\mathbb{P}} = \exp(r_{\mathbb{P}}\,t/4)$ and $\ln(-ix) = \ln(x) - i\pi/2$

Phenomenology: Physical observables

- Total cross-section

$$\sigma_{tot}(s) = \frac{4\pi}{s} \, \text{Im}\, A(s, t=0)$$
$$= X s^{\epsilon} + Y_{+} s^{-\eta_{+}} + \tau \, Y_{-} s^{-\eta_{-}}$$

– where $A(s,t) = A_B(s,t)$ and X and $Y_{\pm}$ represents the imaginary part of the forward scattering amplitude

- Elastic differential cross-section

$$\frac{d\sigma}{d|t|}(s,t) = \frac{\pi}{s^2} \, |\text{Im}\, A(s,t)|^2$$

- Ratio of the real to imaginary part of the forward scattering amplitude

$$\rho(s) = \frac{\text{Re}\, A(s, t=0)}{\text{Im}\, A(s, t=0)}$$

Results so far

	Born-level amplitudes			
	BI	BII	BIII	BI + $\mathbb{PP}$
ϵ	0.0945±0.0035	0.0945±0.0033	0.0958±0.0039	0.0945±0.0038
$\alpha'_{\mathbb{P}}$ [GeV^{-2}]	0.2502±0.0085	0.2495±0.0085	0.3788±0.0088	0.4469±0.0094
$\beta_{\mathbb{P}}(0)$ [GeV^{-1}]	1.949±0.057	1.948±0.052	1.935±0.062	1.950±0.060
$r_{\mathbb{P}}$ [GeV^{-2}]	5.5 [fixed]	5.5 [fixed]	-	5.5 [fixed]
η_+	0.329±0.055	0.329±0.049	0.323±0.059	0.329±0.057
$\beta_+(0)$ [GeV^{-1}]	3.67±0.41	3.66±0.37	3.64±0.44	3.67±0.43
η_-	0.527±0.084	0.527±0.080	0.526±0.090	0.527±0.089
$\beta_-(0)$ [GeV^{-1}]	2.89±0.51	2.89±0.49	2.89±0.54	2.89±0.54
a_1 [GeV^2]	-	m_ρ^2 [fixed]	m_ρ^2 [fixed]	-
a_2 [GeV^2]	-	-	7.5±3.9	-
$\beta_{\mathbb{PP}}(0)$	-	-	-	0.085±0.022
χ^2/dof	0.79	0.79	0.79	0.79
free parameters	7	7	8	8

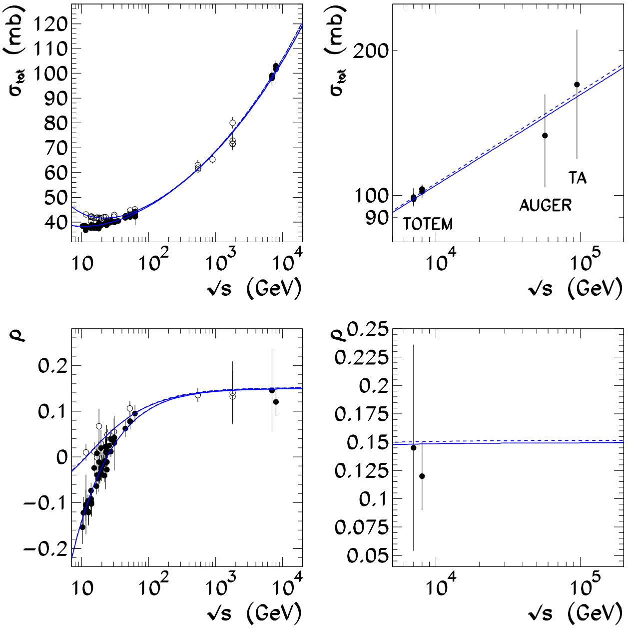

BI, BII *and* BI+$\mathbb{P}\mathbb{P}$ *(continuous curve) and* BIII *(dashed line).*

Phenomenology: Eikonal analysis

- Breakdown of unitarity can be avoided $\rightarrow$ the exchange series

$$\mathbb{P} + \mathbb{P}\mathbb{P} + \mathbb{P}\mathbb{P}\mathbb{P} + \dots$$

- It is not entirely understood how to carry out a full computation of them
- Pomeron contribution $\rightarrow$ **single-exchange** in the Born-level amplitude

Phenomenology: Eikonal analysis

- Breakdown of unitarity can be avoided $\rightarrow$ the exchange series

$$\mathbb{P} + \mathbb{P}\mathbb{P} + \mathbb{P}\mathbb{P}\mathbb{P} + \ldots$$

- It is not entirely understood how to carry out a full computation of them
- Pomeron contribution $\rightarrow$ **single-exchange** in the Born-level amplitude
- Relation one-to-one?

Phenomenology: Eikonal analysis

- Breakdown of unitarity can be avoided $\rightarrow$ the exchange series

$$\mathbb{P} + \mathbb{P}\mathbb{P} + \mathbb{P}\mathbb{P}\mathbb{P} + \ldots$$

- It is not entirely understood how to carry out a full computation of them
- Pomeron contribution $\rightarrow$ **single-exchange** in the Born-level amplitude
- Relation one-to-one?

$$1 - \sum_{n=0}^{\infty} \frac{(i\chi)^n}{n!} = -i\chi + \chi^2 + i\chi^3 + \ldots \leftrightarrow \mathbb{P} + \mathbb{P}\mathbb{P} + \mathbb{P}\mathbb{P}\mathbb{P} + \ldots$$

Phenomenology: Eikonal analysis

- Breakdown of unitarity can be avoided $\rightarrow$ the exchange series

$$\mathbb{P} + \mathbb{P}\mathbb{P} + \mathbb{P}\mathbb{P}\mathbb{P} + \ldots$$

- It is not entirely understood how to carry out a full computation of them
- Pomeron contribution $\rightarrow$ **single-exchange** in the Born-level amplitude
- Relation one-to-one?

$$1 - \sum_{n=0}^{\infty} \frac{(i\chi)^n}{n!} = -i\chi + \chi^2 + i\chi^3 + \ldots \leftrightarrow \mathbb{P} + \mathbb{P}\mathbb{P} + \mathbb{P}\mathbb{P}\mathbb{P} + \ldots$$

- **This is not absolutely true** $\rightarrow$ but it is a phenomenological way to give some meaning to eikonal unitarisation

$$A_B(s,t) = s \int_0^{\infty} db\, b\, J_0(b\sqrt{-t})\, \chi(s,b)$$

– at first order

Phenomenology: Eikonal analysis

- eikonalisation is an effective procedure to take into account some properties of high-energy s-channel unitarity
- inverting the Fourier transform

$$\chi(s,b) = \frac{1}{s}\int_0^{\infty} d\sqrt{-t}\,\sqrt{-t}\,J_0(b\sqrt{-t})\,A_B(s,t)$$

– the first term in the eikonal series is related to the **single-exchange Born-level amplitude**

- the "full eikonalised" amplitude

$$A_{eik}(s,t) = is\int_0^{\infty} db\, b\, J_0(b\sqrt{-t})\left[1 - e^{i\chi(s,b)}\right]$$

– where $\chi(s,b) = \chi_R(s,b) + i\chi_I(s,b)$

Phenomenology: Eikonal analysis

- eikonalisation is an effective procedure to take into account some properties of high-energy s-channel unitarity
- inverting the Fourier transform

$$\chi(s,b) = \frac{1}{s}\int_0^{\infty} d\sqrt{-t}\,\sqrt{-t}\,J_0(b\sqrt{-t})\,A_B(s,t)$$

– the first term in the eikonal series is related to the **single-exchange Born-level amplitude**

- the "full eikonalised" amplitude

$$A_{eik}(s,t) = is\int_0^{\infty} db\,b\,J_0(b\sqrt{-t})\left[1 - e^{i\chi(s,b)}\right]$$

– where $\chi(s,b) = \chi_R(s,b) + i\chi_I(s,b)$

- this is *"""'a way to take into account'""'* the whole multiple-Pomeron exchange

Results so far

	Single-channel eikonalised amplitudes		
	EI	EII	EIII
ϵ	0.1103±0.0020	0.1091±0.0094	0.1213±0.0052
$\alpha'_{\mathbb{P}}$ [GeV^{-2}]	0.2484±0.0010	0.266±0.012	0.1375±0.0057
$\beta_{\mathbb{P}}(0)$ [GeV^{-1}]	2.066±0.012	2.090±0.17	1.917±0.084
$r_{\mathbb{P}}$ [GeV^{-2}]	2.899±0.011	2.56±0.96	-
η_+	0.3563±0.0051	0.360±0.060	0.322±0.054
$\beta_+(0)$ [GeV^{-1}]	4.870±0.056	4.94±0.72	4.56±0.49
η_-	0.5509±0.0027	0.552±0.088	0.544±0.087
$\beta_-(0)$ [GeV^{-1}]	3.760±0.022	3.78±0.70	3.65±0.66
a_1 [GeV^2]	-	m_ρ^2 [fixed]	m_ρ^2 [fixed]
a_2 [GeV^2]	-	-	0.369 ±0.012
χ^2/dof	1.11	1.09	0.80
free parameters	8	8	8

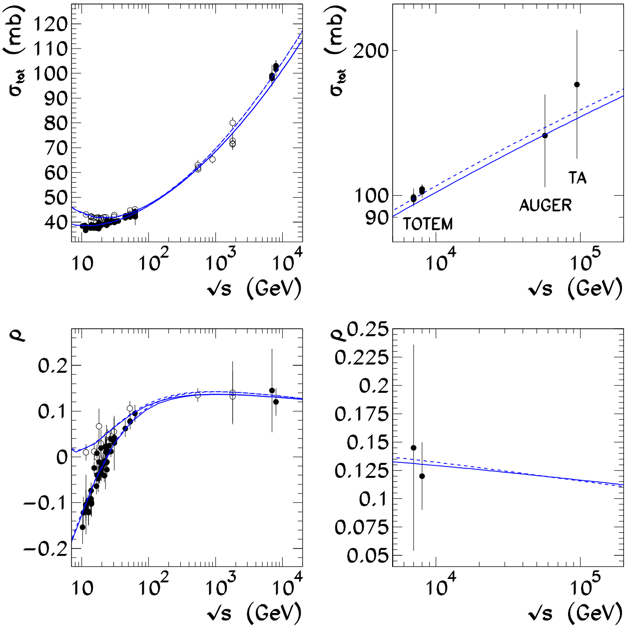

EI *and* EII *(continuous curve) and* EIII *(dashed line).*

Phenomenology: Eikonal analysis

Double-channel eikonal analysis

- Diffractive proton excitation in intermediate states
- two-channel eikonal approach $\rightarrow$ by means of the Good-Walker formalism
  – convenient way to incorporate $p \rightarrow N^*$ diffractive dissociation

$$\beta_p \rightarrow \begin{pmatrix} \beta_p(p \rightarrow p) & \beta_p(p \rightarrow N^*) \\ \beta_p(N^* \rightarrow p) & \beta_p(N^* \rightarrow N^*) \end{pmatrix} \simeq \beta(p \rightarrow p) \begin{pmatrix} 1 & \gamma \\ \gamma & 1 \end{pmatrix}$$

- Pomeron couplings

$$\beta_{\mathbb{P},k}(t) = (1 \pm \gamma)\beta_{\mathbb{P}}(t)$$

  – where $1 \pm \gamma$ stands for the eigenvalues of the two-channel vertex, with $\gamma \simeq 0.55$
  $\rightarrow$ associated with excitations into particular channels with $\sigma_{SD}^{lowM} \simeq 2$ mb at $\sqrt{s} = 31$ GeV
- each amplitude has two vertices

$$A_{eik}(s,t) = is \int_0^\infty b\, db\, J_0(bq) \left[1 - \frac{1}{4}\, e^{i(1+\gamma)^2 \chi(s,b)} - \frac{1}{2}\, e^{i(1+\gamma^2)\chi(s,b)} - \frac{1}{4}\, e^{i(1-\gamma)^2 \chi(s,b)} \right]$$

Results so far

	Two-channel eikonalised amplitudes		
	DI	DII	DIII
ϵ	0.1383±0.0038	0.1393±0.0014	0.1472±0.0044
$\alpha'_{\mathbb{P}}$ [GeV^{-2}]	0.0909±0.00020	0.0703±0.00075	0.0447±0.00048
$\beta_{\mathbb{P}}(0)$ [GeV^{-1}]	1.948±0.027	1.919±0.26	1.896±0.011
$r_{\mathbb{P}}$ [GeV^{-2}]	4.42±0.16	4.787±0.033	-
η_+	0.3314±0.0072	0.3284±0.0055	0.3287±0.0057
$\beta_+(0)$ [GeV^{-1}]	5.261±0.099	5.218±0.039	5.314±0.014
η_-	0.5487±0.0037	0.5475±0.0011	0.5547±0.0022
$\beta_-(0)$ [GeV^{-1}]	4.15±0.50	4.122±0.025	4.165±0.094
a_1 [GeV^2]	-	m_ρ^2 [fixed]	m_ρ^2 [fixed]
a_2 [GeV^2]	-	-	0.383±0.010
χ^2/dof	1.42	1.42	0.85
free parameters	8	8	8

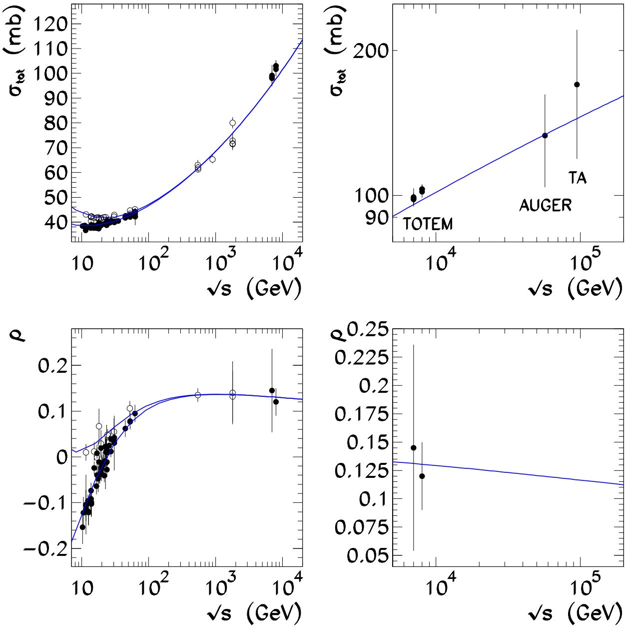

DIII *(continuous curve)*.

Results so far

	BIII model		EIII model		DIII model	
$\sqrt{s}$ [TeV]	σ_{tot} [mb]	ρ	σ_{tot} [mb]	ρ	σ_{tot} [mb]	ρ
7.0	98.9±3.9	0.150±0.006	98.4±3.9	0.135±0.005	96.1±3.8	0.135±0.005
8.0	101.5±7.2	0.150±0.011	100.7±7.2	0.134±0.010	98.4±7.0	0.135±0.010
13.0	111.3±10.2	0.151±0.014	109.3±10.0	0.130±0.012	106.3±9.7	0.135±0.012
14.0	112.9±10.7	0.151±0.014	110.6±10.5	0.130±0.012	107.7±10.3	0.135±0.013
57.0	148±18	0.151±0.019	138±17	0.120±0.015	133±17	0.135±0.017
95.0	163±23	0.151±0.021	149±21	0.116±0.016	144±20	0.135±0.019

Table: Predictions for the forward scattering quantities σ_{tot}^{pp} and ρ^{pp} using different Regge-Gribov based models.

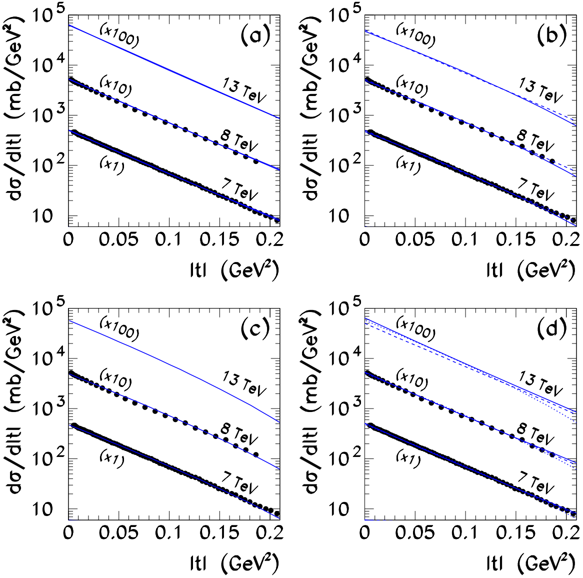

(a) BI, BII *and* BI+$\mathbb{PP}$ *(continuous) and* BIII *(dashed)*; (b) EI *and* EII *(continuous) and* EIII *(dashed); and* (c) *only* DIII. (d) *comparison results among* BIII *(continuous)*, EIII *(dashed) and* DIII *(dotted)*.

Quantum Chromodynamics

QCD: Basics

- Describes the strong interactions among quarks (ψ_q) and gluons (G_μ^A)
- invariant properties of the symmetry group SU(N_c), $N_c = 3$

$$[\lambda^A, \lambda^B] = if^{ABC}\lambda^C$$

- Lagrangian

$$\mathcal{L}_{QCD} = -\frac{1}{4}F^A_{\mu\nu}(x)F_A^{\mu\nu}(x) + \sum_q \bar{\psi}^r_q(x)(i\not{D} - m)_{rs}\psi^s_q(x) + \mathcal{L}_{gauge-fixing} + \mathcal{L}_{ghost}$$

– where
$F^A_{\mu\nu} = \partial_\mu G^A_\nu - \partial_\nu G^A_\mu - g_s f^{ABC} G^B_\mu G^C_\nu$

– $f_{ABE}f_{ECD} + f_{CBE}f_{AED} + f_{DBE}f_{ACE} = 0$

– g_s is the strong coupling

QCD: Basics

- Describes the strong interactions among quarks (ψ_q) and gluons (G^A_μ)
- invariant properties of the symmetry group SU(N_c), $N_c = 3$

$$[\lambda^A, \lambda^B] = i f^{ABC} \lambda^C$$

- Lagrangian

$$\mathcal{L}_{QCD} = -\frac{1}{4} F^A_{\mu\nu}(x) F^{\mu\nu}_A(x) + \sum_q \bar{\psi}^r_q(x)(i\not{D} - m)_{rs}\psi^s_q(x) + \mathcal{L}_{gauge-fixing} + \mathcal{L}_{ghost}$$

– where $F^A_{\mu\nu} = \partial_\mu G^A_\nu - \partial_\nu G^A_\mu - g_s f^{ABC} G^B_\mu G^C_\nu$

– $f_{ABE} f_{ECD} + f_{CBE} f_{AED} + f_{DBE} f_{ACE} = 0$

– g_s is the strong coupling

- Properties:
  - $\Rightarrow$ **Confinement**
  - $\Rightarrow$ **Asymptotic freedom**

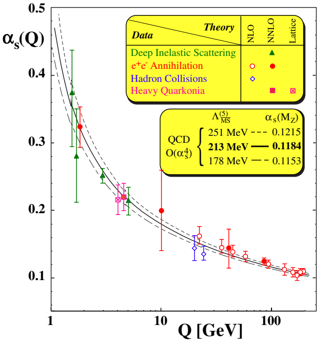

QCD: Basics

- Describes the strong interactions among quarks (ψ_q) and gluons (G^A_μ)
- invariant properties of the symmetry group SU(N_c), $N_c = 3$

$$[\lambda^A, \lambda^B] = if^{ABC}\lambda^C$$

- Lagrangian

$$\mathcal{L}_{QCD} = -\frac{1}{4}F^A_{\mu\nu}(x)F^{\mu\nu}_A(x) + \sum_q \bar{\psi}^r_q(x)(i\not{D} - m)_{rs}\psi^s_q(x) + \mathcal{L}_{gauge-fixing} + \mathcal{L}_{ghost}$$

– where
$F^A_{\mu\nu} = \partial_\mu G^A_\nu - \partial_\nu G^A_\mu - g_s f^{ABC} G^B_\mu G^C_\nu$

– $f_{ABE}f_{ECD} + f_{CBE}f_{AED} + f_{DBE}f_{ACE} = 0$

– g_s is the strong coupling

- Properties:

  $\Rightarrow$ **Confinement**

  $\Rightarrow$ **Asymptotic freedom**

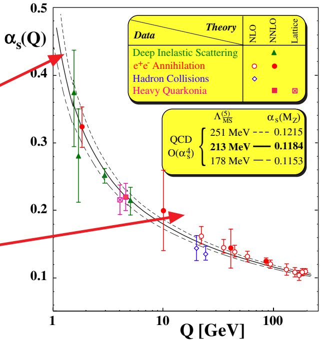

QCD: Effective coupling

- Once it is known $\beta(\alpha_s)$

$$\frac{d\alpha_s(\tau)}{d\tau} = \beta(\alpha_s(\tau)) = Q^2\,\frac{d\alpha_s(Q^2)}{dQ^2} = -b_0\alpha_s^2(Q^2)\left(1 + \frac{b_1}{b_0}\alpha_s(Q^2) + \frac{b_2}{b_0}\alpha_s^2(Q^2) + \ldots\right)$$

- Usually is used LO and NLO terms $\rightarrow$ expansion (only b_0 and b_1 are considered)
- ...

$$\alpha_s^{LO}(Q^2) = \frac{4\pi}{\beta_0 \ln\left(\frac{Q^2}{\Lambda^2}\right)}$$

$$\alpha_s^{NLO}(Q^2) = \frac{4\pi}{\beta_0 \ln\left(\frac{Q^2}{\Lambda^2}\right)}\left[1 - \frac{\beta_1}{\beta_0^2}\,\frac{\ln\ln\left(\frac{Q^2}{\Lambda^2}\right)}{\ln\left(\frac{Q^2}{\Lambda^2}\right)}\right]$$

- $\beta_0 = b_0/4\pi$ e $\beta_1 = b_1/16\pi^2$

QCD: Deep inelastic scattering

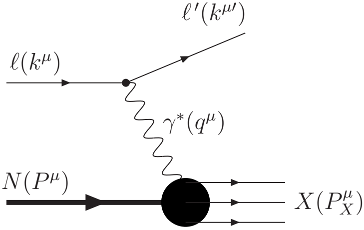

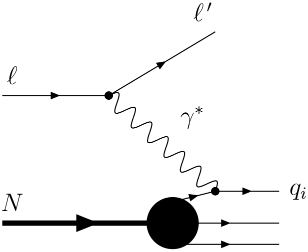

Kinematical variables

- Centre-of-mass $\gamma^* N$ energy squared

$$W^2 = (P+q)^2 \geq m_p^2$$

- Virtuality

$$Q^2 \equiv -q^2 = (k-k')^2 > 0$$

- Bjorken variable, $0 \leq x \leq 1$

$$x = \frac{Q^2}{2p\cdot q} = \frac{Q^2}{Q^2 + W^2 - m_p^2}$$

- Inelasticity, $0 \leq y \leq 1$

$$y = \frac{\nu}{E} = \frac{W^2 + Q^2 - m_p^2}{s - m_p^2}$$

QCD: Parton density

Parton model $\mathcal{O}(\alpha_{em})$

$$F_2 = 2xF_1 = x \sum_i e_i^2 f_i(x)$$

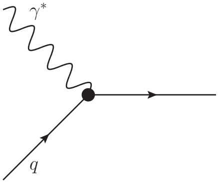

QCD: Parton density

Parton model $\mathcal{O}(\alpha_{em})$

$$F_2 = 2xF_1 = x\sum_i e_i^2 f_i(x)$$

QCD correction $\mathcal{O}(\alpha_s)$

$$F_2(x, Q^2) = \sum_{i=q,\bar{q},g} e_i^2 x f_i(\xi, \mu^2) C^i(z, Q^2, \mu^2)$$

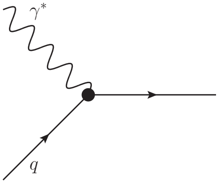

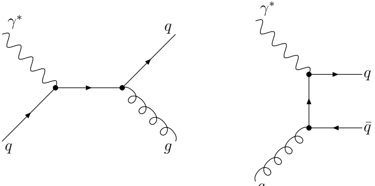

(a) (b)

QCD: Parton density

Parton model $\mathcal{O}(\alpha_{em})$

$$F_2 = 2xF_1 = x\sum_i e_i^2 f_i(x)$$

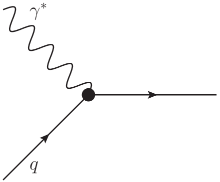

QCD correction $\mathcal{O}(\alpha_s)$

$$F_2(x,Q^2) = \sum_{i=q,\bar{q},g} e_i^2 x f_i(\xi,\mu^2) C^i(z,Q^2,\mu^2)$$

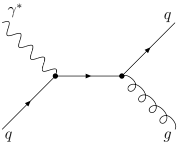

(a)

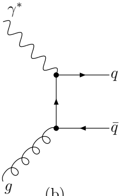

(b)

- DGLAP evolution

$$\frac{\partial\,\mathcal{U}(x,Q^2)}{\partial\ln Q^2} = \frac{\alpha_s}{2\pi}\int_x^1 \frac{d\xi}{\xi}\begin{pmatrix} P_{qq}(z,Q^2) & 2N_f P_{qg}(z,Q^2) \\ P_{gq}(z,Q^2) & P_{gg}(z,Q^2)\end{pmatrix}\begin{pmatrix} f_q(x,Q^2) \\ f_g(x,Q^2)\end{pmatrix}$$

Parton model

Distribution functions

- General hadronic collision $A + B \to C + D$

$$\sigma_{AB\to CD} = \sum_{a,b} \int_{x_a}^{1} d\xi_a \int_{x_b}^{1} d\xi_b\, \hat{\sigma}_{ab}(\xi_a p_A, \xi_b p_B) f_{a/A}(\xi_a) f_{b/B}(\xi_b)$$

- There are many dedicated collaborations which aim to determine the behaviour of the distribution functions
- Here we are using the distributions CTEQ6L, CTEQ6L1 e MSTW2008

$$\text{CTEQ6} \;\Rightarrow xf(x, Q_0) = A_0\, x^{A_1} (1-x)^{A_2}\, e^{A_3 x}\, (1 + e^{A_4}\, x)^{A_5}$$

$$\text{MSTW} \;\Rightarrow xf_i(x, Q_0^2) = A_i x^{-\lambda_i} (1-x)^{\eta_i} (1 + \epsilon_i \sqrt{x} + \gamma_i x)$$

QIM formalism

- Describes some hadronic processes in the interplay between perturbative and non-perturbative region
- the scattering amplitude is written by means of the eikonal formalism

$$\chi(s,b) = \chi_{soft}(s,b) + \chi_{SH}(s,b)$$

$\Rightarrow$ $\chi(s,b) = \chi_R(s,b) + i\chi_I(s,b)$ is the (complex) eikonal function

– we assume that $\chi(s,b)$ for pp and $\bar{p}p$ scatterings are additive with respect to the soft and semi-hard (SH) parton interactions:

$$\chi_{pp}^{\bar{p}p}(s,b) = \chi^+(s,b) \pm \chi^-(s,b)$$

- increase of $\sigma_{tot}(s)$ is directly associated with parton-parton SH scatterings

QIM formalism: The revised DGM

– it follows from the QCD parton model that $\chi_{SH}(s,b)$ factorises as

$$\mathrm{Re}\,\chi_{SH}(s,b) = \frac{1}{2}\, W_{SH}(s,b)\,\sigma_{QCD}(s)$$

- $W_{SH}(b)$ is an overlap density for the partons at impact parameter space b:
- $\sigma_{QCD}(s)$ is the usual QCD cross-section:

$$\sigma_{QCD}(s) = \sum_{ij} \frac{1}{1+\delta_{ij}} \int_0^1 dx_1 \int_0^1 dx_2 \int_{Q^2_{min}}^{\hat{s}/2} d|\hat{t}|\, \frac{d\hat{\sigma}_{ij}}{d|\hat{t}|}(\hat{s},\hat{t}) f_{i/A}(x_1,|\hat{t}|) f_{j/B}(x_2,|\hat{t}|) \Theta\left(\frac{\hat{s}}{2} - |\hat{t}|\right)$$

where $|\hat{t}| \equiv Q^2$ e $i,j = q,\bar{q},g$

- however, the eikonal function

$$\chi^+(s,b) = \chi^+_{soft}(s,b) + \chi^+_{SH}(s,b)$$

$$\chi^-(s,b) = \chi^-_{soft}(s,b) + \chi^-_{SH}(s,b) \simeq \chi^-_{soft}(s,b)$$

QIM formalism: The revised DGM

- The imaginary part of $\chi_{SH}(s,b)$ can be obtained by means of the integral dispersion relation:

$$\text{Im}\,\chi^{+}(s,b) = -\frac{2s}{\pi}\,\mathcal{P}\int_{0}^{\infty} ds'\,\frac{\text{Re}\,\chi^{+}(s',b)}{s'^{2}-s^{2}}$$

- in this way

$$\begin{aligned}
\text{Im}\,\chi_{SH}(s,b) &= -\frac{1}{2\pi}\int_{0}^{\infty} ds'\,\ln\left(\frac{s'+s}{|s'-s|}\right)\left[\sigma_{QCD}(s')\,\frac{dW_{SH}(s',b)}{ds'}\right] \\
&- \frac{1}{2\pi}\int_{0}^{\infty} ds'\,\ln\left(\frac{s'+s}{|s'-s|}\right)\left[W_{SH}(s',b)\,\frac{d\sigma_{QCD}(s')}{ds'}\right] \\
&= I_1 + I_2
\end{aligned}$$

QIM formalism: The revised DGM

- The soft eikonal is needed only to describe the lower-energy forward data
- the main contribution to the asymptotic behaviour of the hadronic total cross-section comes from the partonic SH collisions

⇒ It is enough to build an instrumental parametrization for the soft eikonal:

$$\chi^{+}_{soft}(s,b) = \frac{1}{2}\, W^{+}_{soft}(b;\mu^{+}_{soft}) \left[A' + \frac{B'}{(s/s_0)^{\gamma}}\, e^{i\pi\gamma/2} - iC' \ln\left(\frac{s}{s_0}\right) - i\,\frac{\pi}{2} \right]$$

- The odd term, that accounts for the difference between pp and $\bar{p}p$, channels and vanishes at high energy

$$\chi^{-}_{soft}(s,b) = \frac{1}{2}\, W^{-}_{soft}(b;\mu^{-}_{soft})\, D'\, \frac{e^{-i\pi/4}}{\sqrt{s/s_0}}$$

QIM formalism: The overlap density

- Are written in terms of form factors:

$$
\begin{aligned}
W(b) &= \int d^2b'\, \rho_A(|\mathbf{b}-\mathbf{b}'|)\, \rho_B(b') \\
&= \frac{1}{2\pi}\int_0^\infty dk_\perp\, k_\perp\, J_0(k_\perp b)\, G_A(k_\perp)\, G_B(k_\perp)
\end{aligned}
$$

– $\rho(b)$ is the parton density

- In terms of the form factor it is simply written as:

$$
\rho(b) = \frac{1}{(2\pi)^2}\int d^2k_\perp\, G(k_\perp)e^{i\mathbf{k}_\perp\cdot\mathbf{b}}
$$

- **Simplest hypothesis**: $W_{SH} = W_{soft}$. This prescription is not however true in QCD parton model.

QIM formalism: Energy-dependent form factors

- **Most probable**: a model which quarks and gluons has distinct spatial distributions

QIM formalism: Energy-dependent form factors

- **Most probable**: a model which quarks and gluons has distinct spatial distributions
- The soft overlap densities $W^{-}_{soft}(b)$ and $W^{+}_{soft}(b)$ comes from the dipole approximation to the form factors $G_A(k_\perp)$ and $G_B(k_\perp)$
- thus, using a dipole form factor

$$G_{dip}(k_\perp;\mu) = \left(\frac{\mu^2}{k_\perp^2+\mu^2}\right)^2$$

- one gets

$$\begin{aligned} W^{\pm}_{soft}(b;\mu^{\pm}_{soft}) &= \frac{1}{2\pi}\int_0^\infty dk_\perp\, k_\perp\, J_0(k_\perp b)\, G^2_{dip}(k_\perp;\mu^{\pm}_{soft}) \\ &= \frac{(\mu^{\pm}_{soft})^2}{96\pi}(\mu^{\pm}_{soft} b)^3 K_3(\mu^{\pm}_{soft} b) \end{aligned}$$

QIM formalism: Energy-dependent form factors

- For $W_{SH}(b)$ we consider the possibility of a "broadening" of the spatial distribution of the gluons

⇒ our assumption suggests an increase of the average gluon radius when $\sqrt{s}$ increases

⇒ can be properly implemented using two Ansätze for $W_{SH}(b)$:

$$G_{SH}^{(m)}(s, k_\perp; \nu_{SH}) = \frac{\nu_{SH}^2}{k_\perp^2 + \nu_{SH}^2} \quad \Rightarrow \quad W_{SH}^{(m)}(s, b; \nu_{SH}) = \frac{\nu_{SH}^2}{4\pi}(\nu_{SH} b) K_1(\nu_{SH} b)$$

$$G_{SH}^{(d)}(s, k_\perp; \nu_{SH}) = \left(\frac{\nu_{SH}^2}{k_\perp^2 + \nu_{SH}^2}\right)^2 \quad \Rightarrow \quad W_{SH}^{(d)}(s, b; \nu_{SH}) = \frac{\nu_{SH}^2}{96\pi}(\nu_{SH} b)^3 K_3(\nu_{SH} b)$$

– where $\nu_{SH} = \nu_1 - \nu_2 \ln(s/s_0)$

The δ-function removes the integration over ds'; thus, the second integral can be expressed as

$$
\begin{aligned}
I_2(s,b) &= -\frac{1}{2\pi}\int_0^\infty ds' \ln\left(\frac{s'+s}{|s'-s|}\right) W_{\rm SH}(s',b)\frac{d\sigma_{\rm QCD}(s')}{ds'} \\
&= -\frac{1}{2\pi}\sum_{ij}\frac{1}{1+\delta_{ij}} W_{\rm SH}\left(\frac{2|\hat{t}|}{x_1 x_2}, b\right)\int_0^1 dx_1 \int_0^1 dx_2 \int_{Q^2_{\rm min}}^\infty d|\hat{t}| \frac{d\hat{\sigma}_{ij}}{d|\hat{t}|}(\hat{s},\hat{t}) \\
&\quad \times f_{i/A}(x_1,|\hat{t}|) f_{j/B}(x_2,|\hat{t}|) \ln\left(\frac{\hat{s}/2+|\hat{t}|}{\hat{s}/2-|\hat{t}|}\right)
\end{aligned}
$$

The energy-dependent form factor $W_{\rm SH}(s,b)$ can have a monopole or a dipole form, namely, $W^{(m)}_{\rm SH}(s,b;\nu_{\rm SH})$ or $W^{(d)}_{\rm SH}(s,b;\nu_{\rm SH})$ [see Eqs. (17) and (18)]. In the case of a monopole form, the first integral on the right side of (26) can be rewritten as

$$
\begin{aligned}
I_1^{(m)}(s,b) &= -\frac{1}{2\pi}\int_0^\infty ds' \ln\left(\frac{s'+s}{|s'-s|}\right)\sigma_{\rm QCD}(s')\frac{dW^{(m)}_{\rm SH}(s',b;\nu_{\rm SH})}{ds'} \\
&= -\frac{b}{8\pi^2}\sum_{ij}\frac{1}{1+\delta_{ij}}\int_0^\infty \frac{ds'}{s'}\ln\left(\frac{s'+s}{|s'-s|}\right)\int_0^1 dx_1\int_0^1 dx_2\int_{Q^2_{\rm min}}^\infty d|\hat{t}|\frac{d\hat{\sigma}_{ij}}{d|\hat{t}|}(\hat{s}',\hat{t}) \\
&\quad \times f_{i/A}(x_1,|\hat{t}|) f_{j/B}(x_2,|\hat{t}|)[b\nu_2\nu^3_{\rm SH}K_0(\nu_{\rm SH}b) - 2\nu_2\nu^2_{\rm SH}K_1(\nu_{\rm SH}b)]\Theta\left(\frac{\hat{s}'}{2}-|\hat{t}|\right);
\end{aligned}
$$

in the case of a dipole we get

$$
\begin{aligned}
I_1^{(d)}(s,b) &= -\frac{1}{2\pi}\int_0^\infty ds' \ln\left(\frac{s'+s}{|s'-s|}\right)\sigma_{\rm QCD}(s')\frac{dW^{(d)}_{\rm SH}(s',b;\nu_{\rm SH})}{ds'} \\
&= -\frac{b^3}{192\pi^2}\sum_{ij}\frac{1}{1+\delta_{ij}}\int_0^\infty \frac{ds'}{s'}\ln\left(\frac{s'+s}{|s'-s|}\right)\int_0^1 dx_1\int_0^1 dx_2\int_{Q^2_{\rm min}}^\infty d|\hat{t}|\frac{d\hat{\sigma}_{ij}}{d|\hat{t}|}(\hat{s}',\hat{t}) \\
&\quad \times f_{i/A}(x_1,|\hat{t}|) f_{j/B}(x_2,|\hat{t}|)[b\nu_2\nu^5_{\rm SH}K_2(\nu_{\rm SH}b) - 2\nu_2\nu^4_{\rm SH}K_3(\nu_{\rm SH}b)]\Theta\left(\frac{\hat{s}'}{2}-|\hat{t}|\right).
\end{aligned}
$$

QIM formalism: Infrared mass scale and the role of gluons

- The gluon distribution becomes asymptotically large at $x \to 0$
- in order to obtain $\chi_{sH}(s, b)$ we select parton-parton scattering processes containing **at least one gluon in the initial state**:

$$gg \to gg \;\; \text{(gluon-gluon scattering)}$$
$$qg \to qg \;\; \text{(quark-gluon scattering)}$$
$$\bar{q}g \to \bar{q}g \;\; \text{(quark-gluon scattering)}$$
$$gg \to \bar{q}q \;\; \text{(gluon fusion into a quark pair)}$$

$\Rightarrow$ plagued by infrared divergences

$\Rightarrow$ have to be regularised by means of some cutoff procedure

- one natural regulator for these infrared divergences $\to$ evidence that QCD develops an effective momentum-dependent mass for the gluons
  – this *dynamical* gluon mass mechanism introduces a natural scale

$\Rightarrow$ intrinsically linked to an **infrared-finite QCD effective charge** $\bar{\alpha}_s(Q^2)$

QIM formalism: Infrared mass scale and the role of gluons

- The freezing of the QCD coupling at low energies ***suggests non-perturbative effects***
- a link to dynamical mass generation for gluons $\rightarrow$ were obtained by Cornwall in order to derive a gauge invariant Schwinger-Dyson equation for the gluon propagador

$$\bar{\alpha}_s = \bar{\alpha}_s(Q^2) = \frac{4\pi}{\beta_0 \ln\left[(Q^2 + 4M_g^2(Q^2))/\Lambda^2\right]}$$

$$M_g^2 = M_g^2(Q^2) = m_g^2 \left[\frac{\ln\left(\frac{Q^2 + 4{m_g}^2}{\Lambda^2}\right)}{\ln\left(\frac{4{m_g}^2}{\Lambda^2}\right)} \right]^{-12/11}$$

$\Rightarrow$ $m_g = 500 \pm 200$ MeV

- Perturbative regime is recovered

$$\bar{\alpha}_s(Q^2 \gg \Lambda^2) \sim \frac{4\pi}{\beta_0 \ln\left(\frac{Q^2}{\Lambda^2}\right)} = \alpha_s^{pQCD}(Q^2)$$

QIM formalism: Infrared mass scale and the role of gluons

- **Bearing in mind DGM mechanism**, the parton-parton cross-sections to calculate $\sigma_{QCD}(s)$ are given by

$$\frac{d\hat{\sigma}}{d\hat{t}}(gg \to gg) = \frac{9\pi\bar{\alpha}_s^2}{2\hat{s}^2}\left(3 - \frac{\hat{t}\hat{u}}{\hat{s}^2} - \frac{\hat{s}\hat{u}}{\hat{t}^2} - \frac{\hat{t}\hat{s}}{\hat{u}^2}\right)$$

$$\frac{d\hat{\sigma}}{d\hat{t}}(qg \to qg) = \frac{\pi\bar{\alpha}_s^2}{\hat{s}^2}(\hat{s}^2 + \hat{u}^2)\left(\frac{1}{\hat{t}^2} - \frac{4}{9\hat{s}\hat{u}}\right)$$

$$\frac{d\hat{\sigma}}{d\hat{t}}(gg \to \bar{q}q) = \frac{3\pi\bar{\alpha}_s^2}{8\hat{s}^2}(\hat{t}^2 + \hat{u}^2)\left(\frac{4}{9\hat{t}\hat{u}} - \frac{1}{\hat{s}^2}\right)$$

$\Rightarrow$ at large enough Q^2 these expressions reproduce their pQCD counterparts

- for gluon-gluon process: $\hat{s} + \hat{t} + \hat{u} = 4M_g^2(Q^2)$, whilst for quark-gluon and gluon fusion: $\hat{s} + \hat{t} + \hat{u} = 2M_g^2(Q^2) + 2M_q^2(Q^2)$

$$M_q^2(Q^2) = \frac{m_q^4}{Q^2 + m_q^2} \quad \Rightarrow \quad \text{rapidly decreases with increasing } Q$$

Results so far: Monopole

	CTEQ6L	CTEQ6L1	MSTW
ν_1 [GeV]	1.712 ± 0.541	1.980 ± 0.745	1.524 ± 0.769
ν_2 [GeV]	$(3.376 \pm 1.314) \times 10^{-2}$	$(5.151 \pm 1.627) \times 10^{-2}$	$(9.536 \pm 8.688) \times 10^{-3}$
A' [GeV^{-1}]	125.3 ± 14.7	107.3 ± 9.0	107.2 ± 13.6
B' [GeV^{-1}]	42.96 ± 24.91	28.73 ± 14.78	30.54 ± 16.20
C' [GeV^{-1}]	1.982 ± 0.682	1.217 ± 0.402	1.186 ± 0.466
γ	0.757 ± 0.189	0.698 ± 0.212	0.644 ± 0.250
μ^{+}_{soft} [GeV]	0.777 ± 0.176	0.407 ± 0.266	0.475 ± 0.300
D' [GeV^{-1}]	23.78 ± 1.97	21.37 ± 2.67	21.92 ± 2.83
χ^2/dof	1.060	1.063	1.049

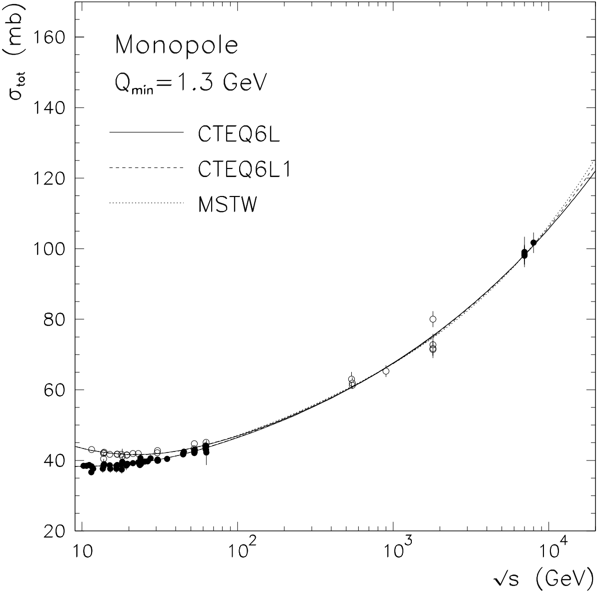

Total cross-section for pp (•) and p̄p (∘).

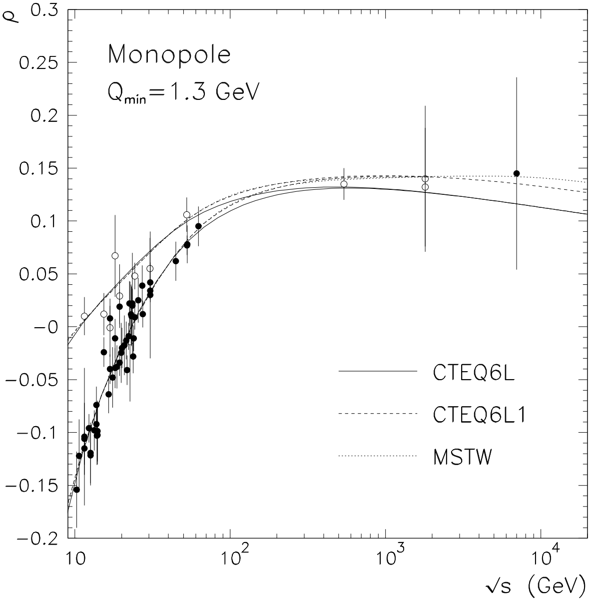

Ratio of the real to imaginary part of the forward scattering amplitude for pp.

Results so far: Dipole

	CTEQ6L	CTEQ6L1	MSTW
ν_1 [GeV]	2.355 ± 0.620	2.770 ± 0.865	2.267 ± 0.845
ν_2 [GeV]	$(5.110 \pm 4.203) \times 10^{-2}$	$(7.860 \pm 5.444) \times 10^{-2}$	$(3.106 \pm 2.920) \times 10^{-2}$
A' [GeV^{-1}]	128.9 ± 13.9	108.9 ± 8.6	108.5 ± 11.5
B' [GeV^{-1}]	46.73 ± 26.13	30.19 ± 15.78	31.63 ± 16.16
C' [GeV^{-1}]	2.103 ± 0.669	1.260 ± 0.437	1.230 ± 0.467
γ	0.780 ± 0.170	0.719 ± 0.200	0.660 ± 0.227
μ^{+}_{soft} [GeV]	0.821 ± 0.150	0.457 ± 0.209	0.506 ± 0.236
D' [GeV^{-1}]	23.96 ± 1.92	21.73 ± 2.26	22.14 ± 2.38
χ^2/dof	1.064	1.062	1.047

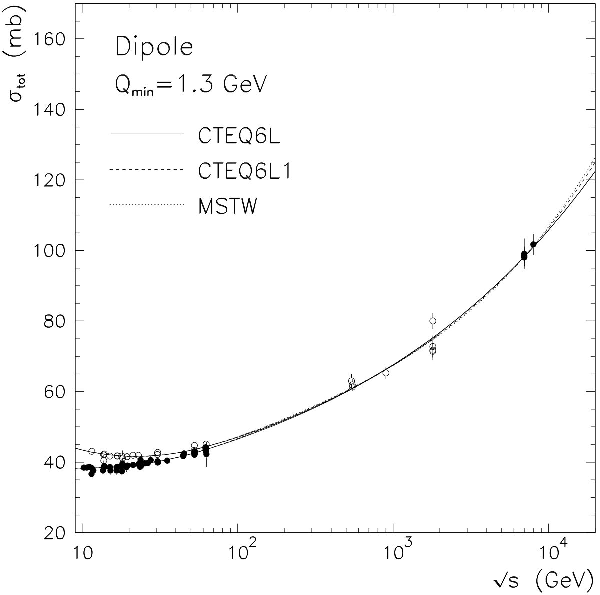

Total cross-section for pp (•) and $\bar{p}$p (○).

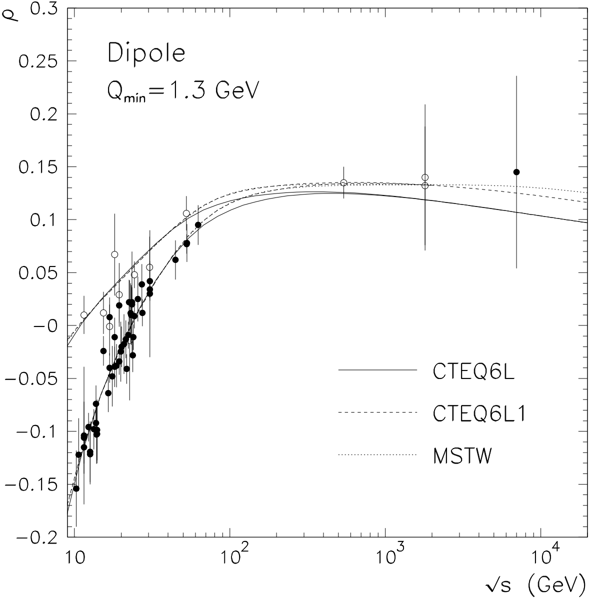

Ratio of the real to imaginary part of the forward scattering amplitude for pp.

	$\sqrt{s}$ [TeV]	σ_{tot} [mb]		ρ	
		monopole	dipole	monopole	dipole
CTEQ6L	8.0	$100.9^{+8.6}_{-7.3}$	$101.0^{+8.6}_{-7.3}$	$0.115^{+0.009}_{-0.008}$	$0.106^{+0.009}_{-0.007}$
	13.0	$111.5^{+9.7}_{-8.4}$	$111.7^{+9.7}_{-8.4}$	$0.110^{+0.010}_{-0.008}$	$0.101^{+0.009}_{-0.008}$
	14.0	$113.2^{+9.9}_{-8.6}$	$113.5^{+9.9}_{-8.6}$	$0.110^{+0.010}_{-0.008}$	$0.100^{+0.009}_{-0.008}$
	57.0	$152.5^{+15.4}_{-14.7}$	$154.1^{+15.6}_{-14.9}$	$0.097^{+0.010}_{-0.010}$	$0.088^{+0.009}_{-0.009}$
	95.0	$170.3^{+17.2}_{-16.5}$	$172.9^{+17.5}_{-16.8}$	$0.092^{+0.010}_{-0.010}$	$0.083^{+0.009}_{-0.009}$
CTEQ6L1	8.0	$101.1^{+8.6}_{-7.3}$	$101.2^{+8.6}_{-7.3}$	$0.134^{+0.012}_{-0.009}$	$0.124^{+0.011}_{-0.009}$
	13.0	$112.4^{+9.8}_{-8.5}$	$112.9^{+9.8}_{-8.5}$	$0.131^{+0.012}_{-0.010}$	$0.120^{+0.011}_{-0.009}$
	14.0	$114.2^{+10.0}_{-8.7}$	$114.9^{+10.0}_{-8.7}$	$0.130^{+0.012}_{-0.010}$	$0.119^{+0.011}_{-0.009}$
	57.0	$159.3^{+16.1}_{-15.4}$	$163.7^{+16.5}_{-15.8}$	$0.117^{+0.012}_{-0.012}$	$0.106^{+0.011}_{-0.011}$
	95.0	$181.5^{+18.3}_{-17.6}$	$188.9^{+19.0}_{-18.4}$	$0.112^{+0.012}_{-0.012}$	$0.101^{+0.011}_{-0.011}$
MSTW	8.0	$101.3^{+8.6}_{-7.3}$	$101.3^{+8.7}_{-7.3}$	$0.142^{+0.013}_{-0.010}$	$0.131^{+0.012}_{-0.009}$
	13.0	$113.3^{+9.9}_{-8.5}$	$113.6^{+9.9}_{-8.5}$	$0.139^{+0.012}_{-0.011}$	$0.128^{+0.011}_{-0.010}$
	14.0	$115.4^{+10.1}_{-8.7}$	$115.7^{+10.1}_{-8.8}$	$0.139^{+0.013}_{-0.011}$	$0.128^{+0.012}_{-0.010}$
	57.0	$162.1^{+16.4}_{-15.6}$	$164.7^{+16.6}_{-15.9}$	$0.127^{+0.013}_{-0.013}$	$0.116^{+0.012}_{-0.011}$
	95.0	$183.0^{+18.5}_{-17.8}$	$187.3^{+18.9}_{-18.2}$	$0.123^{+0.013}_{-0.013}$	$0.112^{+0.012}_{-0.012}$

Table: Predictions for the forward scattering quantities $\sigma_{tot}^{pp,\bar{p}p}$ and $\rho^{pp,\bar{p}p}$.

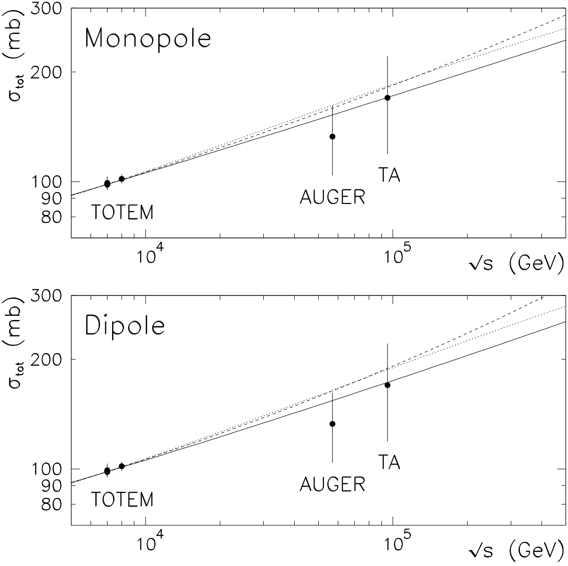

TOTEM, AUGER and Telescope Array (TA) results compared with theoretical expectations obtained using CTEQ6L (solid curve), CTEQ6L1 (dashed curve) and MSTW (dotted curve) parton distribution functions.

Perspectives: On RG-inspired model

- **The signature factor**
  - "the complete expression" for the signature $\eta(t)$
  - within the attempt to cover the whole t-domain

Perspectives: On RG-inspired model

- **The signature factor**
  - "the complete expression" for the signature $\eta(t)$
  - within the attempt to cover the whole t-domain
- **Derivative dispersion relations**
  - *to neglect the real part* of the Born-level amplitude
  - to properly find its correct analytical form by means of a DDR

$$\mathrm{Re}\, A_B(s,t) := \mathrm{DDR}\left[\mathrm{Im}\, A_B(s,t)\right]$$

Perspectives: On RG-inspired model

- **The signature factor**
  - "the complete expression" for the signature $\eta(t)$
  - within the attempt to cover the whole t-domain
- **Derivative dispersion relations**
  - *to neglect the real part* of the Born-level amplitude
  - to properly find its correct analytical form by means of a DDR

$$\mathrm{Re}\, A_B(s,t) := \mathrm{DDR}\left[\mathrm{Im}\, A_B(s,t)\right]$$

- **High-energy ATLAS data** (not mentioned in the text)
  - to study the constraints imposed by ATLAS in the region of high energies

Perspectives: On QCD-inspired model

- **The functional form of the DGM**
  - log- and power-like behaviour
  - different infrared mass scale m_g

Perspectives: On QCD-inspired model

- **The functional form of the DGM**
  - log- and power-like behaviour
  - different infrared mass scale m_g
- **Prescription**
  - to use the *original DGM prescription*

$$\Gamma(s,b) = \left(1 - e^{-\chi(s,b)}\right) \to \left(1 - e^{i\chi(s,b)}\right)$$

Perspectives: On QCD-inspired model

- **The functional form of the DGM**
  - log- and power-like behaviour
  - different infrared mass scale m_g
- **Prescription**
  - to use the *original DGM prescription*

$$\Gamma(s,b) = \left(1 - e^{-\chi(s,b)}\right) \to \left(1 - e^{i\chi(s,b)}\right)$$

- **Derivative dispersion relations**
  - it is ***difficult to implement IDR***

Perspectives: On QCD-inspired model

- **The functional form of the DGM**
  - log- and power-like behaviour
  - different infrared mass scale m_g
- **Prescription**
  - to use the *original DGM prescription*

$$\Gamma(s,b) = \left(1 - e^{-\chi(s,b)}\right) \to \left(1 - e^{i\chi(s,b)}\right)$$

- **Derivative dispersion relations**
  - it is ***difficult to implement IDR***
- **Energy dependence**
  - double-log-like
  - root-log-like
  - the original log-like
- **Experimental data**

Perspectives: On QCD-inspired model

- **The functional form of the DGM**
  - log- and power-like behaviour
  - different infrared mass scale m_g
- **Prescription**
  - to use the *original DGM prescription*

$$\Gamma(s,b) = \left(1 - e^{-\chi(s,b)}\right) \to \left(1 - e^{i\chi(s,b)}\right)$$

- **Derivative dispersion relations**
  - it is ***difficult to implement IDR***
- **Energy dependence**
  - double-log-like
  - root-log-like
  - the original log-like
- **Experimental data**
- **Form factors** (not mentioned in the text)

Articles published in scientific journals

1. **C.A.S. Bahia, M. Broilo and E.G.S. Luna**, *Nonperturbative QCD effects in forward scattering at the LHC*, **Phys.Rev.D92 (2015) no.7 074039.** DOI: 10.1103/PhysRevD.92.074039.
2. **C.A.S. Bahia, M. Broilo and E.G.S. Luna**, *Energy-dependent dipole form factor in a QCD-inspired model*, **J.Phys.Conf.Ser. 706 (2016) no.5 052006.**
   DOI: 10.1088/1742-6596/706/5/052006.
3. **C.A.S. Bahia, M. Broilo and E.G.S. Luna**, *Regge phenomenology at LHC energies*, **Int.J.Mod.Phys. Conf.Ser. vol.45 (2017) 1760064.** DOI: 10.1142/S2010194517600643.
4. **M. Broilo and E.G.S. Luna**, *The soft Pomeron and the LHC data*, **(to be submitted to Physical Review D)**

Back up

Eikonal formalism

- If, however, the profile function is written according to Durand & Pi prescription

$$\Gamma(s,b) = 1 - e^{-\chi(s,b)}$$

- Total cross-section

$$\sigma_{tot}(s) = 4\pi \int_0^\infty db\, b\, [1 - e^{-\chi_R} \cos\chi_I] = \sigma_{el} + \sigma_{in}$$

- ρ-parameter

$$\rho(s) = -\frac{\int_0^\infty db\, b\, e^{-\chi_R} \sin\chi_I}{\int_0^\infty db\, b\, \left(1 - e^{-\chi_R} \cos\chi_I\right)}$$

Regge theory: Convergence domain

- The continuation to complex angular momenta naturally emerges
- At first glance

$$A(s,t) = \sum_{\ell=0}^{\infty}(2\ell+1)\, A_\ell(t) P_\ell(z)$$

– gives the t-channel correct scattering representation

– physical t-channel domain: $t \geq 4m^2$ and $-1 \leq z \leq 1$

– but cannot be used in the limit of high energies as the crossing symmetric amplitude

- The poles are in the $A_\ell(t)$, but the energy-dependence appears in the $P_\ell(z)$
- Asymptotically at $s \to \infty$ the series diverges

Regge theory: Convergence domain

- In the case of real values of ℓ

$$\lim_{\ell \to \infty} P_\ell(\cos\vartheta) = \mathcal{O}(e^{\ell |\mathrm{Im}\,\vartheta|})$$

- partial-wave series converges only if $A_\ell(t)\, e^{\ell |\mathrm{Im}\,\vartheta|} \leq 1$

$$\lim_{\ell \to \infty} A_\ell(t) \sim e^{-\ell \eta(t)}$$

  – the convergence domain for the partial-wave amplitude for $|\mathrm{Im}\,\vartheta| \leq \eta(t)$

- Converge in a domain slightly larger than the physical one, however ***cannot*** be continued to regions where s becomes arbitrarily large

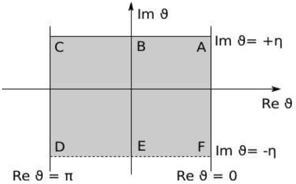

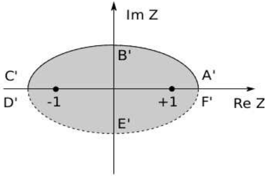

Regge theory: Convergence domain

- In the case of purely imaginary values of ℓ

$$\lim_{\ell \to i\infty} P_\ell(\cos\vartheta) = \mathcal{O}(e^{|\ell||\mathrm{Re}\,\vartheta|})$$

- partial-wave series converges only if $A_\ell(t)\, e^{|\ell||\mathrm{Re}\,\vartheta|} \leq 1$

$$\lim_{\ell \to i\infty} A_{|\ell|}(t) \sim e^{-|\ell|\delta(t)}$$

  – the convergence domain for the partial-wave amplitude for $|\mathrm{Re}\,\vartheta| \leq \delta(t)$

- It has an ***open domain***, and therefore s can become asymptotically large

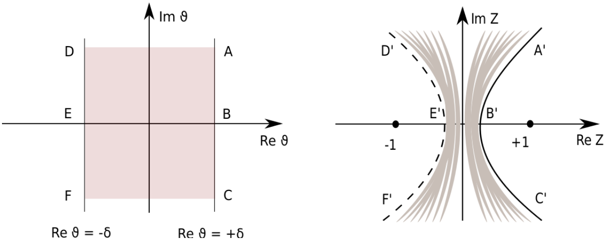

Regge theory: Regge poles

- By applying the Regge theory into relativistic scattering
  – by means of the Froissart-Gribov projection:

$$A_\ell(t) = \frac{1}{\pi}\int_{z_0}^{+\infty} dz_t\, D_s(s(z_t,t),t)\, Q_\ell(z_t) + \frac{1}{\pi}\int_{-z_0}^{-\infty} dz_t\, D_u(u(z_t,t),t)\, Q_\ell(z_t)$$

- The scattering amplitude is written as the **Watson-Sommerfeld** transform of the partial-wave series:

$$\begin{aligned} A(z_t,t) = & -\pi \sum_{\xi=\pm 1}\sum_{i_\xi} \frac{1+\xi e^{-i\pi\ell}}{2}\gamma_{i_\xi}(t)\,(2\alpha_{i_\xi}(t)+1)\,\frac{P_{\alpha_{i_\xi}}(-z_t)}{\sin\pi\alpha_{i_\xi}(t)} + \\ & + \frac{i}{2}\sum_{\xi=\pm 1}\int_{c-i\infty}^{c+i\infty} d\ell\, \frac{1+\xi e^{-i\pi\ell}}{2}(2\ell+1)A(\ell,t)\frac{P_\ell(-z_t)}{\sin\pi\ell}d\ell \end{aligned}$$

- Leading pole $\rightarrow$ **Pomeron** $\xi = +1$

$$A(s,t) \underset{s\to\infty}{\sim} -\gamma_i(t)\,\frac{1+\xi e^{-i\pi\alpha(t)}}{\sin\pi\alpha(t)}\, s^{\alpha(t)}$$

Regge theory: Regge poles

- New quantum number, the signature $\xi = \pm 1$
  – Then $A_\ell(t)$ can be analytically continued to complex ℓ-values by means of the **Watson-Sommerfeld transform**

- The dominant contribution in the case of t-channel exchange

$$A(s,t) \underset{s\to\infty}{\simeq} \sum_{\xi=\pm 1} \sum_{i_\xi} -\gamma_{i_\xi}(t) \frac{1+\xi e^{-i\pi\alpha_{i_\xi}(t)}}{\sin \pi\alpha_{i_\xi}(t)} s^{\alpha_{i_\xi}(t)}$$

– α_{i_ξ} defines the location of the i-th pole $\rightarrow$ each Reggeon contribution
– $\gamma_{i_\xi}(t)$ stands for the residue function and *phenomenologically* is related to the vertex coupling hadron-Reggeon

- **Fundamental result:**

Regge theory: Regge poles

- New quantum number, the signature $\xi = \pm 1$
  – Then $A_\ell(t)$ can be analytically continued to complex ℓ-values by means of the **Watson-Sommerfeld transform**

- The dominant contribution in the case of t-channel exchange

$$A(s,t) \underset{s\to\infty}{\simeq} \sum_{\xi=\pm 1} \sum_{i_\xi} -\gamma_{i_\xi}(t) \frac{1+\xi e^{-i\pi\alpha_{i_\xi}(t)}}{\sin \pi\alpha_{i_\xi}(t)} s^{\alpha_{i_\xi}(t)}$$

  – α_{i_ξ} defines the location of the i-th pole $\rightarrow$ each Reggeon contribution
  – $\gamma_{i_\xi}(t)$ stands for the residue function and *phenomenologically* is related to the vertex coupling hadron-Reggeon

- **Fundamental result:** the leading complex angular momentum singularity of the partial-wave amplitude in a given channel, determines the asymptotic behaviour of the scattering amplitude in the crossed channels

Regge theory: Regge poles

- New quantum number, the signature $\xi = \pm 1$

  – Then $A_\ell(t)$ can be analytically continued to complex ℓ-values by means of the **Watson-Sommerfeld transform**

- The dominant contribution in the case of t-channel exchange

$$A(s,t) \underset{s\to\infty}{\simeq} \sum_{\xi=\pm 1} \sum_{i_\xi} -\gamma_{i_\xi}(t) \frac{1+\xi e^{-i\pi\alpha_{i_\xi}(t)}}{\sin \pi\alpha_{i_\xi}(t)} s^{\alpha_{i_\xi}(t)}$$

  – α_{i_ξ} defines the location of the i-th pole $\rightarrow$ each Reggeon contribution

  – $\gamma_{i_\xi}(t)$ stands for the residue function and *phenomenologically* is related to the vertex coupling hadron-Reggeon

- **Fundamental result:** the ~~leading complex angular momentum singularity~~ **Regge pole** of the partial-wave amplitude in a given channel, determines the asymptotic behaviour of the scattering amplitude in the crossed channels

Regge theory: Regge poles

Almost the whole story

- By applying the Regge theory into relativistic scattering
  – by means of the Froissart-Gribov projection:

$$A_\ell(t) = \frac{1}{\pi}\int_{z_0}^{+\infty} dz_t\, D_s(s(z_t,t),t)\, Q_\ell(z_t) + \frac{1}{\pi}\int_{-z_0}^{-\infty} dz_t\, D_u(u(z_t,t),t)\, Q_\ell(z_t)$$

- The scattering amplitude is written as the **Watson-Sommerfeld** transform of the partial-wave series:

$$\begin{aligned} A(z_t,t) = & - \pi \sum_{\xi=\pm 1}\sum_{i_\xi} \frac{1+\xi e^{-i\pi\ell}}{2}\, \gamma_{i_\xi}(t)\,(2\alpha_{i_\xi}(t)+1)\, \frac{P_{\alpha_{i_\xi}}(-z_t)}{\sin \pi\alpha_{i_\xi}(t)} + \\ & + \frac{i}{2}\sum_{\xi=\pm 1}\int_{c-i\infty}^{c+i\infty} d\ell\, \frac{1+\xi e^{-i\pi\ell}}{2}(2\ell+1)A(\ell,t)\frac{P_\ell(-z_t)}{\sin \pi\ell}\, d\ell \end{aligned}$$

- **Fundamental result:**

Regge theory: Regge poles

Almost the whole story

- By applying the Regge theory into relativistic scattering
  – by means of the Froissart-Gribov projection:

$$A_\ell(t) = \frac{1}{\pi}\int_{z_0}^{+\infty} dz_t\, D_s(s(z_t,t),t)\, Q_\ell(z_t) + \frac{1}{\pi}\int_{-z_0}^{-\infty} dz_t\, D_u(u(z_t,t),t)\, Q_\ell(z_t)$$

- The scattering amplitude is written as the **Watson-Sommerfeld** transform of the partial-wave series:

$$\begin{aligned} A(z_t,t) = \quad & - \quad \pi \sum_{\xi=\pm 1}\sum_{i_\xi} \frac{1+\xi e^{-i\pi\ell}}{2}\, \gamma_{i_\xi}(t)\,(2\alpha_{i_\xi}(t)+1)\, \frac{P_{\alpha_{i_\xi}}(-z_t)}{\sin \pi\alpha_{i_\xi}(t)} + \\ & + \quad \frac{i}{2}\sum_{\xi=\pm 1}\int_{c-i\infty}^{c+i\infty} d\ell\, \frac{1+\xi e^{-i\pi\ell}}{2}(2\ell+1)A(\ell,t)\,\frac{P_\ell(-z_t)}{\sin \pi\ell}\, d\ell \end{aligned}$$

- **Fundamental result:** the leading complex angular momentum singularity of the partial-wave amplitude in a given channel, determines the asymptotic behaviour of the scattering amplitude in the crossed channels

Regge theory: Regge poles

Almost the whole story

- By applying the Regge theory into relativistic scattering
  - by means of the Froissart-Gribov projection:

$$A_\ell(t) = \frac{1}{\pi}\int_{z_0}^{+\infty} dz_t\, D_s(s(z_t,t),t)\, Q_\ell(z_t) + \frac{1}{\pi}\int_{-z_0}^{-\infty} dz_t\, D_u(u(z_t,t),t)\, Q_\ell(z_t)$$

- The scattering amplitude is written as the **Watson-Sommerfeld** transform of the partial-wave series:

$$A(z_t,t) = -\pi \sum_{\xi=\pm1}\sum_{i_\xi} \frac{1+\xi e^{-i\pi\ell}}{2}\gamma_{i_\xi}(t)\,(2\alpha_{i_\xi}(t)+1)\,\frac{P_{\alpha_{i_\xi}}(-z_t)}{\sin\pi\alpha_{i_\xi}(t)} + \\ + \frac{i}{2}\sum_{\xi=\pm1}\int_{c-i\infty}^{c+i\infty} d\ell\, \frac{1+\xi e^{-i\pi\ell}}{2}(2\ell+1)A(\ell,t)\frac{P_\ell(-z_t)}{\sin\pi\ell}d\ell$$

- **Fundamental result:** the **Regge pole** ~~leading complex angular momentum singularity~~ of the partial-wave amplitude in a given channel, determines the asymptotic behaviour of the scattering amplitude in the crossed channels

Phenomenology: Physical observables

$$\text{(BI)}\quad \sigma_{tot}^{pp,\bar{p}p} = 18.382\, s^{0.0945} + 57.298\, s^{-0.329} \mp 30.097\, s^{-0.527}$$

$$\text{(BII)}\quad \sigma_{tot}^{pp,\bar{p}p} = 18.364\, s^{0.0945} + 56.986\, s^{-0.329} \mp 30.097\, s^{-0.527}$$

$$\text{(BIII)}\quad \sigma_{tot}^{pp,\bar{p}p} = 18.114\, s^{0.0958} + 56.664\, s^{-0.323} \mp 30.053\, s^{-0.526}$$

$$\text{(BI+}\mathbb{PP}\text{)}\quad \sigma_{tot}^{pp,\bar{p}p} = 18.401\, s^{0.0945} + 57.298\, s^{-0.329} \mp 30.097\, s^{-0.527} - \\ - 3.381 \times 10^{-2}\, s^{1.189}\, \mathrm{Im}\left[\frac{i}{\ln s - i\frac{\pi}{2}}\right]$$

QCD: Effective coupling

- Processes contributing to the appearance of divergences
- field rescaling $\rightarrow$ **redefinition** of physical quantities (renormalisation)

$$g_s \;\rightarrow\; \alpha_s(\mu) = \frac{g_s^2}{4\pi}$$

- renormalisation group equation:

$$\left(-\frac{\partial}{\partial\tau} + \beta(\alpha_s)\,\frac{\partial}{\partial\alpha_s}\right)\mathcal{R}(e^{\tau},\alpha_s) = 0$$

– $\mathcal{R}(e^{\tau},\alpha_s) = \mathcal{R}(1,\alpha_s(\tau)) = \alpha_s(\tau)$ is solution with boundary condition $\alpha_s(\tau=0) = \alpha_s(\mu^2) = \alpha_s$

- ...

$$\tau = \int_{\alpha_s(0)}^{\alpha_s(\tau^2)} \frac{d\alpha'}{\beta(\alpha')} \quad , \quad \frac{d\alpha_s(\tau)}{d\tau} = \beta(\alpha_s(\tau)) \quad , \quad \frac{d\alpha_s(\tau)}{d\alpha_s} = \frac{\beta(\alpha_s(\tau))}{\beta(\alpha_s)}$$

- scale-dependence is in α_s

QIM formalism

- In this approach the energy dependence of the $\sigma_{tot}(s)$ is obtained from the QCD using an eikonal formulation

- More specifically: behaviour of the forward observables $\sigma_{tot}(s)$ and $\rho(s)$ derived from the QCD parton model

$\Rightarrow$ standard QCD cross-sections for elementary parton-parton processes

$\Rightarrow$ updated sets of quark and gluon distribution functions

$\Rightarrow$ physically-motivated cutoffs which restrict the parton-level processes to semi-hard (SH) ones

- SH processes arise from hard scatterings of partons carrying very small fractions of the momenta of their parent hadrons

$\Rightarrow$ appearance of jets with $E_T \ll \sqrt{s}$

QIM formalism

- In this picture the scattering of hadrons is an incoherent summation over all possible constituent scattering

$\Rightarrow$ increase of $\sigma_{tot}(s)$ is directly associated with parton-parton semi-hard scatterings

$\Rightarrow$ The high-energy dependence of $\sigma_{tot}(s)$ driven mainly by processes involving the gluon contribution

- The nonperturbative character of the QCD is also manifest at the elementary level...

$\Rightarrow$ At high energies the soft and the semi-hard components of the scattering amplitude are closely related

QIM formalism

- Task of describing $\sigma_{tot}(s)$ and $\rho(s)$ bringing up information about the infrared properties of QCD

$\Rightarrow$ can be properly addressed by considering the possibility that the nonperturbative dynamics of QCD generate an effective gluon mass

$\Rightarrow$ The dynamical gluon mass is intrinsically related to an infrared finite strong coupling constant

$\Rightarrow$ its existence is strongly supported by recent QCD lattice simulations as well as by phenomenological results

- With this backgorund in mind, our main purpose is to explore the nonperturbative dynamics of QCD in order to describe the total cross-section and the ρ-parameter.

QIM formalism: The dynamical gluon mass model

- In the eikonal representation:

$$\sigma_{tot}(s) = 4\pi \int_0^\infty b\, db\, [1 - e^{-\chi_R(s,b)} \cos \chi_I(s,b)]$$

$$\sigma_{inel}(s) = \sigma_{tot}(s) - \sigma_{el}(s) = 2\pi \int_0^\infty b\, db\, [1 - e^{-2\chi_R(s,b)}]$$

$$\rho(s) = \frac{-\int_0^\infty b\, db\, e^{-\chi_R(s,b)} \sin \chi_I(s,b)}{\int_0^\infty b\, db\, [1 - e^{-\chi_R(s,b)} \cos \chi_I(s,b)]}$$

– $\chi(s,b) = \chi_R(s,b) + i\chi_I(s,b)$ is the (complex) eikonal function

Results so far

- We carried out a global fit to high-energy forward pp and $\bar{p}p$ scattering data above $\sqrt{s} = 10$ GeV

⇒ we have included the recent data at LHC from the TOTEM Collaboration

⇒ we used a χ^2 fitting procedure as our statistical indicator, assuming an interval $\chi^2 - \chi^2_{min}$, in the case of normal errors, to the projection of the χ^2 hypersurface containing 90% of probability

⇒ we have investigated the effects of some updated sets of parton distributions on the high-energy cross-sections, namely CTEQ6L, CTEQ6L1 and MSTW

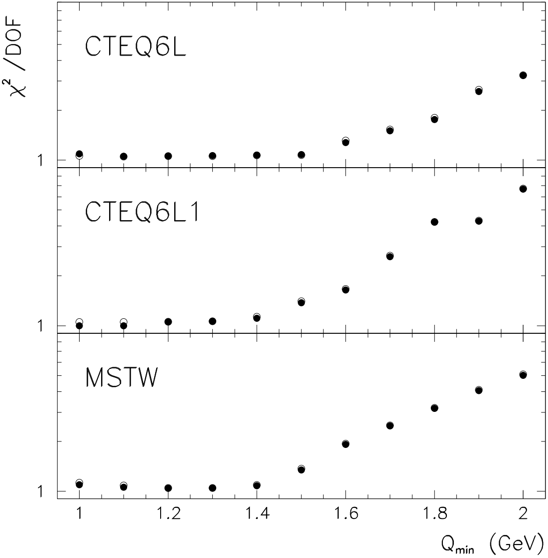

The χ^2/dof as a function of the cutoff Q_{min} for the monopole (○) and the dipole (●) semi-hard form factor.

Results: Partial conclusions on QIM

- The model introduces a natural IR cutoff
- The dynamical gluon mass M_g and the strong coupling $\bar{\alpha}_s$ are *physically well motivated*
- Recent lattice QCD simulations $\rightarrow$ clear evidence for the dynamical generation of a gluon mass
- The frozen coupling $\bar{\alpha}_s$ provides an **useful phenomenological tool** to the study of processes where a purely perturbative QCD method is inadequate
- The main contribution is that with our model we were able to study in details the $\sigma_{tot}(s)$ and $\rho(s)$.